ASTROBIOLOGY
Volume 7, Number 1, 2007

DOI: 10.1089/ast.2006.0108

Special Paper

Spectral Signatures of Photosynthesis. II. Coevolution with Other Stars and the Atmosphere on Extrasolar Worlds

NANCY Y. KIANG,[1,2] ANTÍGONA SEGURA,[2,3] GIOVANNA TINETTI,[2,4] GOVINDJEE,[5] ROBERT E. BLANKENSHIP,[6] MARTIN COHEN,[2,7] JANET SIEFERT,[2,8] DAVID CRISP,[2,9] and VICTORIA S. MEADOWS[2,10]

Apparently the vegetable kingdom in Mars, instead of having green for a dominant colour, is of a vivid blood-red tint.

—H.G. Wells, *The War of the Worlds,* 1898

ABSTRACT

As photosynthesis on Earth produces the primary signatures of life that can be detected astronomically at the global scale, a strong focus of the search for extrasolar life will be photosynthesis, particularly photosynthesis that has evolved with a different parent star. We take previously simulated planetary atmospheric compositions for Earth-like planets around observed F2V and K2V, modeled M1V and M5V stars, and around the active M4.5V star AD Leo; our scenarios use Earth's atmospheric composition as well as very low O_2 content in case anoxygenic photosynthesis dominates. With a line-by-line radiative transfer model, we calculate the incident spectral photon flux densities at the surface of the planet and under water. We identify bands of available photosynthetically relevant radiation and find that photosynthetic pigments on planets around F2V stars may peak in absorbance in the blue, K2V in the red-orange, and M stars in the near-infrared, in bands at 0.93–1.1 μm, 1.1–1.4 μm, 1.5–1.8 μm, and 1.8–2.5 μm. However, underwater organisms will be restricted to wavelengths shorter than 1.4 μm and more likely below 1.1 μm. M star planets without oxygenic photosynthesis will have photon fluxes above 1.6 μm curtailed by methane. Longer-wavelength, multi-photosystem series would reduce the quantum yield but could allow for oxygenic photosystems at longer wavelengths. A wavelength of 1.1 μm is a possible upper cutoff for electronic transi-

[1]NASA Goddard Institute for Space Studies, New York, New York.
[2]NASA Astrobiology Institute–Virtual Planetary Laboratory.
[3]Instituto de Ciencias Nucleares, Universidad Nacional Autónoma de México, México City, México.
[4]Institut d'Astrophysique de Paris, European Space Agency, Paris, France.
[5]Departments of Plant Biology and Biochemistry, University of Illinois at Urbana-Champaign, Urbana, Illinois.
[6]Department of Biology and Chemistry, Washington University, St. Louis, Missouri.
[7]Radio Astronomy Laboratory, University of California, Berkeley, Berkeley, California.
[8]Department of Statistics, Rice University, Houston, Texas.
[9]NASA Jet Propulsion Laboratory, Pasadena, California.
[10]Spitzer Science Center, California Institute of Technology, Pasadena, California.

tions versus only vibrational energy; however, this cutoff is not strict, since such energetics depend on molecular configuration. M star planets could be a half to a tenth as productive as Earth in the visible, but exceed Earth if useful photons extend to 1.1 μm for anoxygenic photosynthesis. Under water, organisms would still be able to survive ultraviolet flares from young M stars and acquire adequate light for growth. Key Words: Photosynthesis—Astrobiology—Photosynthetic pigments—Oxygenic photosynthesis—Anoxygenic photosynthesis—Atmospheric photochemistry—F stars—G stars—Sun—K stars—M stars—AD Leo—Atmospheric oxygen—Atmospheric radiative transfer—Chlorophyll—Bacteriochlorophyll—Photosystems—Radiation spectrum—Photosynthetically active radiation—Light harvesting—Modeling—Extrasolar planets—Earth-like planets—Virtual Planetary Laboratory—Biosignatures. Astrobiology 7(1), 252–274.

1. INTRODUCTION: PLANET FINDING MISSIONS, BIOSIGNATURES OF PHOTOSYNTHESIS ON EARTH, AND LITERATURE REVIEW ON EXTRASOLAR PHOTOSYNTHESIS

ALTHOUGH WE NOW KNOW that Mars has no surface vegetation (we have not yet ruled out other life), H.G. Wells was nonetheless prescient in speculating that photosynthetic organisms on another planet might evolve to have a different dominant color than the green that is prevalent on Earth. Over 200 giant planets in other solar systems have been discovered since 1993. In August 2004, the discovery of three Neptune-mass planets via the radial velocity technique (Butler *et al.*, 2004; McArthur *et al.*, 2004) pushed the lower mass limit of discovered planets down from gas giants like Jupiter to close to those of the smaller ice giant planets in our Solar System. The microlensing technique has also led to the recent discovery of a 13 Earth-mass planet (Gould *et al.*, 2006), implying that they are common. The recent discoveries of a 7.5 Earth-mass planet (Rivera *et al.*, 2005) and a 5.5 Earth-mass planet around M dwarf stars (Beaulieu *et al.*, 2006) have provided the first indications of what may be rocky "terrestrial" planets orbiting a main sequence star.

The techniques used for these discoveries are unlikely to detect planets of Earth's mass around other stars. Space telescope missions will be required to take that final step, and in the next 10–20 years, we will not only find terrestrial planets of comparable size to the Earth [via the transit method with NASA's Kepler mission (Borucki *et al.*, 2003; Basri *et al.*, 2005) and the ESA's Corot mission (Bordé *et al.*, 2003)], but also obtain spectra from them [via coronagraphic and interferometry techniques with NASA's Space Interferometry Mission, Terrestrial Planet Finder (Beichman *et al.*, 1999), and the ESA's Darwin mission (Leger, 2000)]. Scientists will need to determine how to interpret those spectra for signs of life. Although life abounds in hidden places of the Earth, independent of sunlight, such as at hydrothermal vents (Karl *et al.*, 1980; Campbell *et al.*, 2001) and 3–4-km-deep metabasalt fractures (Lin *et al.*, 2006), photosynthetic organisms, in particular, are the basis for nearly all life on Earth and produce some of the strongest indicators of life in abundances that can be detected astronomically.

Indicators of photosynthetic life include both distinct reflectance spectra of the organisms and gaseous products that are primarily biogenic in origin. The characteristic reflectance spectra of photosynthesizers result from the combination of pigments that preferentially absorb light in particular wavelengths and the spectral effects produced by the macrostructure of the organisms. The dominant such spectral signature on Earth is that of green plants, which absorb in the visible over about 400–700 nm, with slightly lower absorbance in the green. A stronger signature than the "green bump" is a high reflectance in the near-infrared (NIR) over about 700–850 nm, which causes a steep contrast between the visible and NIR reflectance in the red, the "red edge" (Tucker, 1976; Grant, 1987).

The notable gaseous product of photosynthesis is oxygen, the result of the splitting of water molecules [biochemistry (Rutherford and Boussac, 2004) and atmospheric O_2 buildup (Catling *et al.*, 2001; Sleep, 2001); reviewed by Wydrzynski and Satoh, 2005)]. The Earth's abundant atmospheric oxygen concentration is the result of the long-term balance against geochemical sinks (Kasting, 2001). Although oxygen can be pro-

duced abiotically through photolysis and the net effects of carbon burial and hydrogen escape, it is still a strong biomarker, since the significant buildup of oxygen in a planet's atmosphere and its simultaneous presence with reduced gases are unlikely without production by complex biotic processes that maintain such atmospheric chemical disequilibrium (Lovelock, 1965; Leger *et al*., 1999). Other biogenic gases exist, some being direct products from organisms, such as certain volatile organic compounds emitted by plants (Guenther *et al*., 1995; Kesselmeier and Staudt, 1999), and some being secondary products, such as O_3 from photolysis of O_2 and nitric oxides (NO_x), N_2O, CH_3Cl, and COS from the breakdown of organic matter (Schlesinger, 1997; Watts, 2000). Except for NO_x, which has a short atmospheric lifetime and comparable abiogenic sources (Wayne, 1991), these compounds could be potential biomarkers. However, the "red edge" and oxygen remain the primary indicators of life as they result directly during the process of photosynthesis itself. Could photosynthesis arise on another planet? And if so, would it exhibit the same kind of surface spectral signature as well as the same gaseous products as on Earth?

Previous workers have examined the question of photosynthesis on extrasolar planets and its detectability. Seager *et al*. (2005) reviewed the various early spectroscopic investigations that ruled out the seasonal darkening on Mars as due to vegetation, based on comparison to chlorophyll and red edge spectra. Franck *et al*. (2001) and Cockell and Raven (2004) reviewed the limits of habitability for photosynthesis, from extreme environments to favorable, protective microhabitats, such as crystalline rocks that shield against ultraviolet (UV) radiation. Wolstencroft and Raven (2002) concluded that oxygenic photosynthesis on other planets is indeed plausible, even for different types of parent stars with different radiation spectra and flux densities. Heath *et al*. (1999) examined in particular the distribution of temperature and radiation zones suitable for Earth-like plant photosynthesis on the surface of tidally locked planets around M dwarfs. They identified climatic regions that are favorable and summarized potential adaptations for survival or even utilization of UV flares. A number of workers have proposed that phototrophy utilizing H_2S could exist in clouds on Venus (Sagan, 1961; Grinspoon, 1997; Schulze-Makuch *et al*., 2002, 2004). Woolf *et al*. (2002), Arnold *et al*. (2002), Montañes-Rodriguez *et al*. (2004, 2005), and Seager *et al*. (2005) examined the Earthshine spectrum (the Moon's reflectance of the Earth's radiance) as an example of a planetary disk-averaged spectrum that might be seen by the Terrestrial Planet Finder. Oxygen is abundant enough in the atmosphere to be clearly observed in the Earthshine. Ozone and the oxygen dimer, O_4, are more difficult to detect, but present. Some of these observations show that the contrast caused by the red edge in the Earth's disk-averaged reflectance spectrum is significant enough to indicate the presence of vegetation, while Montañes-Rodriguez *et al*. (2005) found the red edge obscured by clouds. A model of Earth's disk-averaged radiance spectrum by Tinetti *et al*. (2006b) indicates that vegetation must cover at least 20% of the planet's cloud-free surface to be detectable. While the "red edge" is the main reflectance signature for photosynthesis on Earth, Wolstencroft and Raven (2002) postulated that extrasolar vegetation may have photosynthetic pigments adapted to different stellar types, possibly utilizing more photons per carbon fixed, such that we must also be prepared for the possibility of an "edge" that is not red. Seager *et al*. (2005), therefore, advocated that efforts to detect photosynthesis on extrasolar planets take into account the possibility of edge-like signatures, but at other (unknown) wavelengths, in combination with biosignature gases, such as O_2 and O_3 (Leger *et al*., 1993, 1999; Lawson *et al*., 2004). Tinetti *et al*. (2006c) took the suggestion of Wolstencroft and Raven (2002) that oxygenic photosynthesis could utilize three photons instead of two and posed a hypothetical extrasolar vegetation reflectance spectrum for planets around M stars by shifting an Earth vegetation reflectance spectrum so that the edge is in the NIR. They found that an edge-like feature in the NIR could be easier to detect through clouds in a CO_2-rich atmosphere—as they simulated for a planet orbiting an M star—but harder to detect in an Earth-like atmosphere. More studies need to be done to determine whether such edge-like features are biologically reasonable in the NIR.

The above work has established the plausibility of oxygenic photosynthesis and its detectability on extrasolar planets, and acknowledges the possibility of alternative surface spectral signatures of photosynthetic organisms adapted to other radiation regimes. Here, we will extend this work to explore in more detail the coevolution of photosynthesis—not only oxygenic but also anoxy-

genic—with a different atmosphere and parent star, and we will identify how we might predict reasonable (or rule out unreasonable) surface photosynthetic spectral signatures consistent with another planetary environment. This is the next step toward discerning likely photosynthetic signatures for extrasolar planets. With upcoming space telescope missions designed to detect and characterize planets, a better understanding of how photosynthesis could coevolve with different atmospheres and parent stars is needed to interpret the data and will help to develop a strategy for the selection of stars for detailed observation.

Our overarching tenets are these: the light spectrum incident at a planet's surface is a function of not only the parent star's light spectrum, but also the medium through which it is transmitted—the atmospheric or water environment. Further, the spectral transmittance of these media is a function of biogenic inputs that influence the composition of the media with further alterations by photochemistry or other biotic and chemical transformations. Because life alters its environment, the properties of photosynthetic organisms may be partially a result of their own products or those of their predecessors. Therefore, characterization of the light regime for photosynthesis must consider spectral radiation as transmitted through a medium altered by biogenic inputs.

In this paper, we (1) formulate specific rules for the above themes for searching for extrasolar photosynthetic surface spectra, (2) identify plausible combinations of parent star, atmospheric composition, surface gas flux, and photosynthetic pigment properties, (3) model the surface incident photon flux densities for these scenarios, (4) identify wavelengths for likely peak pigment absorbance and bands for photosynthetically active radiation (PAR), and (5) quantify the potential global productivity of extrasolar photoautotrophs.

2. PRINCIPLES FOR PHOTOSYNTHETIC PIGMENT ADAPTATION TO DIFFERENT PARENT STARS AND ATMOSPHERES

To pose plausible combinations of photosynthetic pigment spectra, parent star, atmospheric composition, and surface gas flux, and to address what to look for in extrasolar photosynthetic biosignatures, we need to consider and extend our understanding of Earth-based photosynthesis. In a companion paper (Kiang *et al*., 2007), we reviewed pigment and surface reflectance properties across the range of Earth's photosynthetic organisms, from anoxygenic purple bacteria to vascular plants. We related these spectra to the mechanisms of light harvesting and the spectral light environment of these organisms. We observed how photosynthetic pigment spectra are strongly correlated with features of the incident photon flux spectrum, such as oxygen and water vapor bands in the atmosphere, and NIR transmittance through other organisms in murky water depths. In that review, we thus proposed rules to explain the wavelengths at which photosynthetic pigments have their peak absorbance on Earth.

To extend those rules now for photosynthesis on extrasolar planets, we need to accommodate the possibility that either anoxygenic or oxygenic photosynthesis might dominate on a planet. With regard to the latter, Wolstencroft and Raven (2002) proposed that, on planets with little visible light, oxygenic photosynthesis could be achieved by the utilization of more photons at longer wavelengths. We elaborate next on how this might be possible.

2.1. Potential for oxygenic photosynthesis at longer wavelengths

Several workers have observed that the potential for oxygen production, while limited on Earth principally to photosystems that operate in the 400–700 nm range, can theoretically extend to utilization of lower-energy photons at a wavelength as long as 1,400–1,500 nm if three or four photons are used instead of the current two in Photosystem I (PS I) and II (PS II) of oxygenic photosynthesis (Hill and Bendall, 1960; Hill and Rich, 1983; Heath *et al*., 1999; Wolstencroft and Raven, 2002). The main requirement is that $+479.1$ kJ mol^{-1} of chemical energy be stored to allow for $CO_2 + H_2O \rightarrow (1/6)$ glucose $+ O_2$. How could the higher quantum use be achieved?

The Z-scheme of Earth-based oxygenic photosynthesis (see Fig. 1 in Kiang *et al*., 2007) demonstrates how photosystems linked in series can use more than one photon to achieve the necessary redox spans between the ground and excited states of reaction centers to generate reduced product. Furthermore, the oxidation of water does not depend on the wavelengths of the pho-

tons used. Instead, it relies on the potential difference of water from the oxygen-evolving complex and P680, the reaction center of chlorophyll of PS II, a difference that results from their molecular configuration. Since redox span, rather than reaction center midpoint redox potential, is what constrains the photon wavelength that is useful, there is no reason sufficient redox spans for generation of reduced product cannot theoretically be achieved by chaining more photosystems together (*i.e.*, a multiple Z-scheme) that utilize lower-energy photons. The efficiency would be influenced by the amount of illumination and losses to favor forward over backward reactions. It may be that a reaction center relative to an extrasolar oxygen-evolving complex cannot achieve a sufficiently high midpoint redox potential without some configuration that absorbs only more energetic photons. To date, however, we know of no theoretical constraint. So it would not be beyond an extrasolar photosynthesizer, as far as we know, to evolve other kinds of electron carriers to accommodate a higher quantum requirement.

The efficiency of conversion of light energy to chemical energy in photosynthesis implies that there is no clear upper bound to wavelengths that could be used in photosynthesis. Currently, four photons work in concert in PS II to oxidize $2H_2O$ to evolve an O_2 (Krishtalik, 1986; Tommos and Babcock, 2000; Ferreira *et al.*, 2004; McEvoy *et al.*, 2005), and these are then matched with four photons in PS I, such that a minimum of eight photons total are necessary for fixation of one CO_2. The simultaneous action of the four photons on the oxygen-evolving complex is much more favorable energetically than if they operated one at a time. The energy input by these eight photons is (by Planck's Law) 1,387.2 kJ mol^{-1}, if 680 nm is used in PS II (1,339.0 V if 730 nm). The efficiency of energy input for typical plant photosynthesis is 479.1/(1,339.0 to 1,387.0), or ~35%, and in typical conditions, with some unsuccessful photons and some used for cyclic photophosphorylation and nitrogen assimilation [leading to up to 12 photons used (Govindjee, 1999)], the efficiency is closer to 27% (Blankenship, 2002). The Calvin-Benson cycle is about 90% efficient in carbon fixation (Blankenship, 2002). The light reactions could theoretically approach nearly 100% availability of the photon energy, if illuminated with a mode-locked laser [but more typically, in Earth-like conditions and due to thermal equilibrium between ground and excited states of ensembles of reaction centers, about two-thirds of the photon energy is available for use (Parson, 1978)]. It is possible that an extrasolar photosynthesizer could achieve higher (or lower) efficiency.

Some efficiency limits might be set by losses from activation energies and configurational energy losses (Krishtalik, 1986, 2003). Also, at some long enough wavelength the photons could fail to provide electronically useful states and induce only vibrational energy and no electronic transitions, which would place an upper bound on eligible wavelengths. Above 1,100 nm, radiation is all thermal, or at least cannot be measured using optical sensors, and this may be one possible upper limit. So far, we cannot precisely define what that limit is, as it depends on the molecular configuration. Quantification of this physical limit would be a good subject for a future study.

Therefore, a three-photosystem series that utilizes wavelengths up to about 1,040 nm could provide the same energy input as the two PS II and PS I systems in the visible. A four-photosystem series that utilizes wavelengths up to about 1,400 nm could also provide that same energy input, as could a six-photosystem series that utilizes wavelengths up to 2,100 nm. These would be equivalent to quantum requirements of, in order, 12–18, 16–24, and 24–36 photons per CO_2 fixed, or perhaps there might be a mix of these.

Similarly, one can infer photosystem sequences utilizing other electron donors with other minimum potential difference requirements for electrochemical decomposition. Thus, there is the possibility of multiple chaining of photosystems to perform oxygenic photosynthesis at longer wavelengths. Given no clear physical limit to useful wavelengths, the constraints may be primarily the spectral availability of radiation. We now extend our rules for the Earth to constrain plausible extrasolar photosynthetic biosignatures.

2.2. Rules for plausible photosynthetic biosignatures

2.2.1. Surface incident spectral photon flux densities. The light regime for photosynthesis must be characterized by the incident spectral *photon* flux density, not by the spectral *energy* flux density of solar radiation, because photosynthetic light harvesting and electron donor oxidation rely on the number of photons, not the total energy. The spectral photon flux will determine bands for

PAR. On Earth, PAR is a term generally used to refer to the 0.4–0.7 μm band used by plants, but we extend it more broadly to mean any radiation used for photosynthesis, including purple bacteria that absorb in the NIR as well as extrasolar photosynthesis.

Figure 1a reproduces spectra from Segura *et al*. (2003, 2005) of radiation flux incident on the top of the atmosphere of Earth-like planets that have an average surface temperature of 288 K in orbits around observed F2V and K2V stars, for the active M4.5V star AD Leo, and for modeled quiescent M stars with effective temperatures of 3,100 K and 3,650 K (M5V and M1V), respectively. In addition, the flux spectrum of the Sun incident at the top of the Earth's atmosphere is shown (source is the solar spectrum used in Tinetti *et al.*, 2006a). The fluxes below 280 nm were not plotted because these wavelengths are not considered photosynthetically active and the surface fluxes at these short wavelengths are either negligible with an ozone shield on F, G, and K star planets, or very small on M star planets (Segura *et al*., 2005, Fig. 10). Figure 1a shows the energy flux density, whereas Fig. 1b shows the photon flux density, which dramatizes the difference in using one spectrum versus the other to speculate on pigment adaptations. The Sun's peak energy flux density at the top of the Earth's atmosphere occurs at 450 nm, whereas its peak photon flux density occurs at 572–584 nm. In Kiang *et al*. (2007), we showed how the surface incident spectral *photon* flux density is shifted even more to the red to peak at 670–680 nm. This could explain why chlorophyll favors the red and why plant reflectance in the green is not due to suboptimal use of solar energy.

2.2.2. Photosynthetic pigments. Photosynthetic pigments are adapted to suit several constraints: light harvesting within the available incident photon flux spectrum and oxidation–reduction potential differences to generate reduced product. In Kiang *et al*. (2007), we proposed an explanation as to why chlorophyll and other pigments favor particular wavelengths, and our rationale can be applied to other planets. In particular, photosynthetic pigments would have their absorbance peaks in these wavelength categories:

1. The wavelength of peak incident photon flux within a radiation transmittance window, as the main environmental pressure.

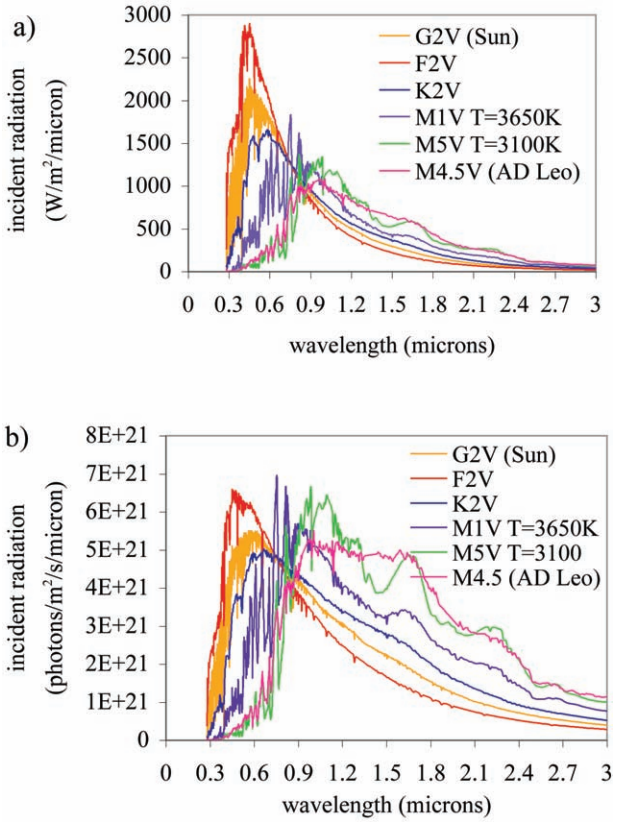

FIG. 1. Top-of-the-atmosphere incident radiation for F2V, G2V (Sun), K2V, M1V, M4.5V, and M5 stars, in terms of (a) energy units (reproduced from Segura *et al*., 2005) and (b) photon flux densities.

2. The longest wavelength within a radiation window for core antenna or reaction center pigments, due to the resonance transfer of excitation energy and an energy funneling effect from shorter to longer wavelengths.
3. The shortest wavelengths within an atmospheric window for accessory pigments, also due to resonance transfer.

The energy per photon may limit the useful wavelength range over which sufficient redox potential differences can be achieved by the excited state of a photosynthetic reaction center; however, as we pointed out earlier, we cannot yet propose a rule for a theoretical upper limit.

2.2.3. Whole-organism reflectance. Reflectance spectra of whole organisms derive from both pigment absorbance spectra and the macrostructure (*e.g*., cell structure, leaf morphology, canopy structure) of the organism adapted for other survival needs (*e.g*., climate and chemical environ-

ment). The whole-organism reflectance spectrum is what ultimately can be observed by remote detection.

In our review of photosynthetic reflectance spectra (Kiang *et al*., 2007), we were not able to draw conclusions about the functional role of a whole organism's reflectance spectrum besides pigment influences. The variability of the red edge and the high reflectance of plants in the NIR are not well understood as adaptations for survival, yet this is thus far the principal empirical means used to identify the presence of plants. We found the NIR reflectance not to be universally the same among all photosynthetic organisms, with a sloping "edge" for lichens, an NIR edge in purple bacteria, and trends across taxa in the wavelength at which NIR reflectance begins to plateau in the red edge, from reddest for terrestrial vascular plants, to bluer for more primitive organisms like mosses and lichens, and bluest for snow algae. More research is needed to explain these trends. A weak or sloping spectral reflectance would challenge the detectability of a reflectance signature, and given a lack of understanding about Earth-based organisms, we cannot yet conjecture whole-organism reflectance spectra for extrasolar photosynthesis.

2.2.4. Biogenic inputs influence the light spectrum. Biogenic products and, in particular, oxygen will influence the spectral transmittance of the atmosphere or water bodies. On an extrasolar planet, either oxygenic or anoxygenic photosynthesis might dominate, and oxygenic photosynthesis is possible with longer than visible wavelengths, as described earlier. Planets around cooler stars that emit little visible light could still possibly produce oxygen as a biosignature of photosynthesis. On the other hand, anoxygenic photosynthesis was the earliest form on the early Earth (Olson, 2006) and, if abundant at the global scale on another planet, could lead to a very different atmospheric composition and surface spectral signature.

We listed biogenic gases earlier: O_2, NO_x, N_2O, CH_3Cl, COS. In addition, CH_4 can be biogenic. These gases are not exclusively biogenic, but on Earth, biota and their by-products are their major sources. The photochemistry and spectral transmittance of these gases, particularly the impact of oxygen, ozone, and UV on their abundance, should be taken into account in examining light spectra available for photosynthesis.

2.2.5. Detectability depends on productivity. Detectability of photosynthesis depends on productivity, which depends on available resources: light, water, electron donors, and nutrients. We will be concerned here with the occurrence of photosynthesis on extrasolar planets that will be both abundant and distinct enough from other confounding spectra to be detectable. Extreme environments and favorable microenvironments could support photosynthesis; however, photosynthesis at these extremes and in these hidden niches would not likely be productive enough to be detectable with a mere disk-averaged resolution of a planet, as will be available from space telescopes like the Terrestrial Planet Finder and Darwin. Therefore, we focus on photosynthetic processes that can plausibly be widespread over a planet's surface.

Low global productivity by anaerobic organisms (Canfield *et al*., 2006) may make these organisms difficult to detect with regard to the magnitude of their trace gas fluxes. Their surface spectra, on the other hand, could be detectable given enough biomass buildup. Anaerobic metabolisms may have difficulty obtaining enough energy to support multicellular organisms (Catling *et al*., 2005) and, hence, to achieve abundant enough biomass to be detectable. However, multicellular, anaerobic worms that live on a sulfur cycle exist in some aquatic environments (Woyke *et al*., 2006). This worm does not live completely independently of oxygen, as the sulfate it uses must come from aerobic respiration by some of its microbial symbionts. Although on Earth there is no multicellular photosynthetic autotroph using sulfide rather than water as the reductant, it is not clear that one could not emerge on another planet. Until we know precisely the energetic constraints to multicellular structure for autotrophs, we will assume the plausibility of complex anoxygenic plant life on land.

To summarize, given the parent star photon flux spectrum and the atmospheric and water spectral transmittance as influenced by biogenic inputs from either oxygenic or anoxygenic photosynthesis, we can identify plausible wavelengths at which extrasolar photosynthetic pigments would peak in absorbance. There is no clear physicochemical upper limit to wavelengths useful for oxygenic photosynthesis, but the limits would most likely be ecological. We cannot predict the whole organism's spectral reflectance signature, given the lack of enough understand-

ing about Earth organisms, but the pigment spectra can allow us to estimate how productive photosynthesis might be on an extrasolar planet. We next consider what to expect on these other planets.

3. EXPECTED CHARACTERISTICS OF PHOTOSYNTHESIS ON TERRESTRIAL PLANETS AROUND F, K, AND M STARS

The star types considered long-lived enough to support a habitable zone capable of evolving life are, in order of decreasing average temperature, F, G, K, and M stars, of which our Sun is a G star. By habitable zone, we mean the range of orbital distances from a star that will allow for the existence of liquid water on a planet (Hart, 1978; Kasting *et al*., 1993). We focus on terrestrial-type planets, since the existence of life forms on gas giants requires speculation beyond analogous examples on Earth.

Figure 1 shows that F stars emit relatively more UV radiation than the Sun, and K stars relatively slightly less UV and visible radiation. Main sequence M stars (also known as M dwarfs or red dwarfs; there also exist non–main sequence M giants) are of interest, because they are the most abundant stars in our galaxy, and they are spectrally much more different from our Sun than F and K stars. They are strongly non-blackbody emitters, with little flux of visible radiation and instead peaking in the NIR. About a quarter of M stars in their early life stage show high amounts of UV radiation and X-rays produced by flares and chromospheric activity, while quiescent stars without flares emit negligible UV radiation (Segura *et al*., 2005). These flares pose potential danger to early organisms. Because of their dimness, the habitable zone of M stars is very close to the star (Kasting *et al*., 1993), such that planets may become tidally locked [one side constantly facing the star (Joshi *et al*., 1997)]. These differing radiation regimes of the F, K, and M stars lead to different atmospheric photochemistry (Segura *et al*., 2005) as well as a much different light spectrum for photosynthesis.

Contrasting scenarios are possible for detectable photosynthesis on extrasolar planets orbiting these stars. Since visible light from F and K stars is of comparable abundance to that on Earth, though shifted slightly in spectrum, oxygenic photosynthesis is likely to be the successful and dominant mode of photosynthesis. The dominant color of photosynthetic organisms might be different for various reasons: (1) the visible spectral flux densities are shifted, favoring peak absorbance at the wavelength of peak flux, with both downhill and uphill excitation energy transfer taking advantage of the available light; (2) some other accident of evolution could lead to phycobilin-type pigments occurring in surface photosynthesizers; and (3) the color could be exactly the same, because of the nature of energy funneling from the bluest, most energetic wavelengths to the redder wavelengths in the reaction centers, and the only difference might be in relative ratios of pigments at these ends.

On M stars with little visible but relatively high NIR radiation, oxygenic photosynthesis may still be plausible, with either low productivity utilizing visible wavelengths or photosystems that utilize longer wavelengths of light and perhaps more photons per O_2 evolved. Anoxygenic photosynthesis could possibly emerge onto land surfaces, since most M stars emit little UV radiation or reduce flare activity after their early stage, and the bulk of the photosynthetically relevant radiation is in the infrared, so an ozone shield or screening pigments against UV would not be necessary. Indeed, anoxygenic photosynthesis could be the dominant form of photosynthesis, if there were abundant non-H_2O electron donors. Photosynthetic organisms on planets around active M stars with high UV flares (the UV can also come from the chromosphere during no flare activity) could have adaptations to survive flare disturbances; some of these adaptations have been observed in Earth organisms (*e.g*., protective pigments, regenerative capacity, life cycles timed to avoid disturbances). There will be little need to protect against UV radiation from quiescent stars.

4. METHODS: MODELED SURFACE INCIDENT PHOTON FLUXES, SCENARIOS FOR F, G, K, AND M STARS, AND ESTIMATION OF PRODUCTIVITY

To conjecture about alternative photosynthetic pigment spectra on extrasolar planets, we modeled the surface radiation regime of terrestrial planets within the habitable zone around F, G, K, and M stars, given atmospheric compositions that might result from a planet dominated by anoxygenic or oxygenic photosynthesis. Models, plau-

sible scenarios, and an approach to compare productivity potential are described below.

4.1. Models: coupled atmospheric photochemical/radiative-convective model, and line-by-line radiative transfer model to calculate surface incident spectral photon flux density

Segura *et al*. (2003, 2005) modeled the impacts of radiation from F, K, and M stars on atmospheric photochemistry of terrestrial planets orbiting these stars. Where they used their simulations to examine the atmospheric profiles of temperature, ozone, and other gases, and then to generate the radiance spectra of the planet as might be observed from space, we employed here the atmospheric compositions generated in their papers to look at the radiation spectrum transmitted through these atmospheres to the surface of the planet.

Briefly, we summarize their model and parameters. For stellar radiation emission, Segura *et al*. (2003, 2005) utilized observed spectra of an F2V star (σ-Bootis, HD 128167), a K2V star (ε-Eridani, HD 22049), and two observed active M stars (AD Leo and GJ643C) and modeled quiescent M stars with effective temperatures of 3,100 K and 3,650 K (Fig. 1a). For a baseline case, they placed an Earth-size planet in the habitable zone and chose the semimajor axis of the planetary orbit to achieve a planetary average surface temperature of 288 K, assuming a rotating planet. The one-dimensional photochemical model (Pavlov and Kasting, 2002) and a radiative-convective model (Pavlov *et al*., 2000) were coupled in Segura *et al*. (2003, 2005) to model atmospheric profiles of temperature, H_2O, O_3, N_2O, CH_4, CO, and CH_3Cl for atmospheres with O_2, CO_2, and N_2 mixing ratios like present-day Earth [present atmospheric level (PAL)] at a surface pressure of 1 atmosphere. The surface trace gas fluxes necessary to achieve these mixing ratios on present Earth were calculated; these surface gas fluxes were then used for further simulations equilibrated with prescribed O_2 mixing ratios. In the case of M stars, only the 1 PAL of O_2 atmosphere was studied. The planets around *active* M stars have the same boundary conditions as the planets around F, G, and K stars. For those planets around *quiescent* M stars, the boundary conditions on the photochemical model had to be changed to avoid methane runaway (for details, see Segura *et al*., 2005). Given the resulting atmospheric compositions, Segura *et al*. (2003, 2005) then used a high-resolution radiative transfer model, SMART (Meadows and Crisp, 1996; Crisp, 1997), to calculate the radiance spectra of these planets.

So, to examine scenarios of oxygenic and anoxygenic photosynthesis, we utilized the atmospheric compositions that Segura *et al*. (2003, 2005) simulated. Instead of calculating the planet's emitted radiance spectrum, we used the SMART model to calculate the spectral photon flux densities at the surface of the planet. For underwater photosynthesis, we calculated photon fluxes at different water depths, using water spectral transmittance from Segelstein (1981), Sogandares and Fry (1997), and Kou *et al*. (1993), as used in Kiang *et al*. (2007).

4.2. Scenarios: F, G, K, and M stars, 1 PAL O_2 and 10^{-5} PAL O_2

Table 1 shows the modeled configurations that we study here, with two oxygen scenarios and five different stars. For the oxygen concentrations, we used from Segura *et al*. (2003, 2005) the Earth-like mixing ratios (1 PAL) and lowest O_2 mixing ratio, 10^{-5} PAL of O_2, which was the lowest stable concentration in the coupled model (with little UV from the parent star to generate O_3 and, hence, OH to destroy methane, and with-

Table 1. Model Scenarios: Prescribed Conditions, Oxygen Levels, and Parent Stars

Prescribed conditions	*Photosynthesis scenarios*	*Parent stars*
• 288 K Earth-size planet surface temperature • Other gases: CO_2, CH_4, N_2O, CO calculated surface fluxes for present Earth mixing ratios (1 PAL)	1. Oxygenic photosynthesis (O_2 = 1 PAL mixing ratio) 2. Anoxygenic photosynthesis (O_2 = 10^{-5} PAL O_2)	1. F2V observed 2. K2V observed 3. M4.5V known active: AD Leo 4. M5V modeled quiescent: T = 3,100 K 5. M1V modeled quiescent: T = 3,650 K

out another modeled methane sink, it is possible to get "runaway methane" in the model).

For the F and K stars, we looked at the 1 PAL atmosphere, and for the M stars, since O_2 largely absorbs in the visible and there is little visible radiation, we looked at the 1 PAL and 10^{-5} PAL O_2 atmospheres for anoxygenic scenarios. We did not examine intermediate mixing ratios of O_2, since they do not lend more insight into the light spectrum for photosynthesis. Also, the transition between the two extreme states is likely to be rapid, such that the planet spends little time in the intermediate states (James Kasting, personal communication).

In these scenarios, although we calculate other surface trace gas fluxes, we did not attempt to calculate net surface fluxes of O_2 or estimate oxygenation times for the planetary atmospheres, given the range of possibilities for photosynthetic efficiencies and respiration and the unknowns of carbon burial and crustal oxidation rates (Sleep, 2001; Catling *et al*., 2005). The prescribed O_2 mixing ratios used by Segura *et al*. (2003, 2005) were sufficient for our purposes. Also, though full ecosystem processes—not only oxygen fluxes from photosynthesis, but also products of decomposition and other biogeochemical transformations—have a net impact on the atmosphere, we did not vary the fluxes of other biogenic gases, since quantification of these sources is poor for the Earth. It also turns out that, except for methane, these other gases do not have significant absorption bands at wavelengths below 1,100 nm, and only methane and N_2O have absorption bands that could be photosynthetically relevant between 1,100 and 2,500 nm. Methane's sources could be both biogenic and abiogenic, and variation of its fluxes could be the subject of a future study on the redox balance of extrasolar planets. Focusing on just different oxygen scenarios provided enough variation in surface photon flux spectra for us to identify likely pigment characteristics and compare productivity potentials of different planets.

4.3. Global average photosynthetic photon flux densities (PPFDs) and productivity

To check the accuracy of the PPFD calculations, we compared values for the Earth. Zhang *et al*. (2004) estimated the Earth's average annual 400–700 nm PPFD per surface area as 3.1×10^{20} photons/m^2/s for clear sky conditions and 2.4×10^{20} photons/m^2/s including cloud cover data (they calculated shortwave radiation with a three-dimensional general circulation model and with satellite and ground data; we converted their shortwave radiation to visible PAR using a PAR/shortwave surface energy flux fraction from Lean and Rind (1998) and mol/J using 485 nm as an average PAR wavelength). This is equal to a 24% reduction of surface visible radiation by clouds. Ito and Oikawa (2004), in a model of global net primary productivity (NPP) using another cloudiness data set, estimated 2.1×10^{20} photons/m^2/s average surface PPFD (352.2 J/year over 1.323×10^8 km^2 of vegetated area), about 12.5% lower than Zhang *et al*. (2004). This may indicate a bias of clouds over vegetation. From these spectra, we posit alternative photosynthetic pigment spectra and bands of PAR.

To estimate potential productivity, as it is beyond the scope of this paper to address full ecosystem dynamics in detail, we focused on the productivity and pigment spectra of photolithoautotrophic photosynthesizers, which are "primary producers" that harvest light energy and fix carbon from CO_2, rather than heterotrophic photosynthesizers that consume already reduced carbon products. The potential autotrophic productivity depends on the actual light availability at the planet's surface, influenced by clouds. We approximated the average noontime PPFD for the illuminated face of a cloudless planet by the PPFD at a solar zenith angle of 60° from the vertical planet's surface. To simulate night, we used half the time-averaged PPFD with cloud cover (for non–tidally locked planets). Since we do not know how clouds on other planets will differ from those on Earth, we estimated the global average cloudy PPFD by reducing the time- and disk-average PPFD values by 24% from Zhang *et al*. (2004) to obtain the average global non–cloud-free PPFD.

We extrapolated from Earth's land versus ocean light use efficiencies for net CO_2 fixation at the global scale. The maximum quantum yield for photosynthesis (both oxygenic and anoxygenic) is 1/8 carbon per photons absorbed, or 0.125. Taking into account possibly 12 photons total to include cyclic electron flow and nitrogen assimilation, the quantum yield is 0.083. Not all incident PAR photons get utilized for photosynthesis, however, because of environmental variability

and resource limitations (water, nitrogen, soil nutrients). On Earth, gross primary productivity (GPP)—GPP is defined by biogeochemists as the gross amount of carbon fixed excluding respiration—on land ranges from 90 to 120 Pg-C/year (Cramer, 1999) for an ice-free land area of 1.32×10^{14} km^2 (about 26% of the Earth's surface). Ocean productivity is approximately the same, but spread over 71% of the Earth's surface. Ocean productivity, in fact, is the main contributor to atmospheric oxygen through carbon burial. The annual surface incident PAR (400–700 nm) of 2.6×10^{20} photons/m^2/s gives then an average quantum yield of just 0.006 fixed CO_2 per incident PAR photon for land and 0.002 for the ocean. The NPP (gross fixed carbon minus autotrophic respiration) is about half the gross, but as respiration is very imprecisely understood, we will look just at GPP, which relates directly to photons used.

Given these efficiencies and assuming similar resource constraints (at least relatively) on other planets, the CO_2 fluxes from GPP can be compared for the different planets. We calculated this potential productivity but not net CO_2 flux from the surface, as we did not have enough information to estimate geochemical processes, such as carbon burial and crustal oxidation rates, and we did not calculate soil microbial respiration (Raich and Schlesinger, 1992; Grace and Rayment, 2000). We assumed Earth-like ice-free land cover and ocean surface area. Productivity also varies by climate zones (Joshi *et al*., 1997), but our back-of-the-envelope global estimates, like those of Wolstencroft and Raven (2002), were adequate for comparing the model scenarios in lieu of modeling surface spatial heterogeneity.

5. RESULTS: SPECTRAL SURFACE AND UNDERWATER INCIDENT PHOTON FLUX DENSITIES AND WAVELENGTHS OF PEAK PHOTON FLUX

Figure 2 shows the incident photon flux densities for the top of the atmosphere, the surface maximum, and the surface-illuminated face average for the F, K, and M stars. The wavelengths of peak surface photon flux are indicated, as well as major gas absorption features. Segura *et al*. (2005) analyzed the radiance spectra for biogenic gas signatures in the UV, the visible and up to 1.6 μm, and in the infrared over 5–20 μm. In general, the 1.6–3.0 μm region is not very radiant and, therefore, difficult to observe, but for interest, our plots show the photon flux spectra up to 3 μm. The plot for the F2V planet in Fig. 2a indicates bands where O_2, O_3, H_2O, and CO_2 absorb, with these bands common to all the 1 PAL scenarios. For all cases, H_2O strongly divides the available radiation into clearly defined windows. In the oxygenic scenarios, the oxygen A-band at 0.761 μm and B-band at 0.687 μm also possibly demarcate window boundaries, and in Kiang *et al*. (2007), we proposed that these are the boundaries for the chlorophyll reaction center in PS II and its absorbance tail in the red edge NIR plateau. These transmittance windows are labeled in Fig. 2b: U, for UV wavelengths 0.280–0.400 μm; V, visible and Earth PAR, 0.400–0.761 μm; W, 0.761–0.934 μm; X, 0.934–1.135 μm; Y, 1.135–1.350 μm; Z, 1.470–1.840 μm; and Q, 1.840–2.5 μm. The cutoffs between the W, X, Y, and Z windows are set where the photon flux reaches a minimum. The K2V planet's surface spectra in Fig. 2b show the same absorbance features as the F2V planet, since the parent star spectra impact the atmospheric photochemistry similarly. Primarily, the O_3 Chappuis band, weakly absorbing over ~0.5 to ~0.7 μm, has differing impacts on the two planets' surface spectra, based on its placement relative to the peak incident stellar radiation. On the F2V planet, it causes the peak photon flux to be biased more strongly toward the blue, whereas on the K2V planet, it shifts the peak more toward the red, as for the Earth (Kiang *et al*., 2007).

On the planets around M stars, Segura *et al*. (2005) noted that the low UV flux results in high CH_4 concentrations, as can be seen in their infrared spectra. In addition, in Fig. 2c–e, we see CH_4 absorption at ~1.6–1.8 μm and at 2.3–2.4 μm, cropping the Z and Q windows for the M star planets. Furthermore, N_2O shows its signature at three places between 2.1 μm and 2.3 μm in the M star oxygenic scenarios (but not in the anoxygenic M star, or F2V and K2V scenarios). If photons at these wavelengths longer than 1.1 μm are relevant to photosynthesis, then on planets around M stars, methane and nitrous oxide will alter the PAR spectrum and impact pigment properties. N_2O could be a strong biomarker at the 2.1 μm band, given that methane is ambiguous as a biomaker.

Given the above atmospheric transmittances, Fig. 3 indicates the wavelengths of peak photon flux and approximate window edges at solar

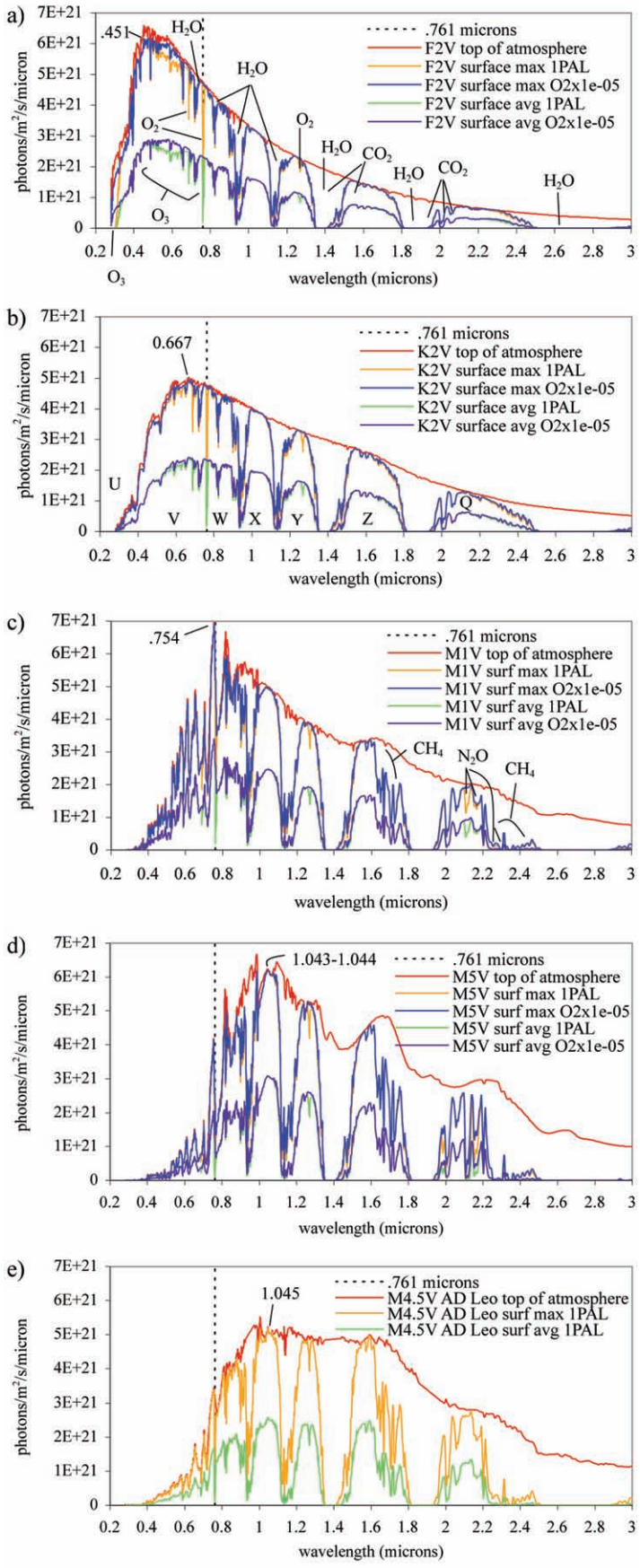

FIG. 2. Incident spectral photon flux densities at the top of the atmosphere, at the surface at the equator at solar noon, and for the surface-illuminated face, clear-sky average for an Earth-like planet with Earth's PAL (1 PAL) of oxygen and other biogenic gas surface fluxes, as well as with atmospheric oxygen at 10^{-5} PAL. Planetary atmospheres were calculated by Segura *et al*. (2003, 2005) for the following parent star types: (**a**) F2V, (**b**) K2V, (**c**) M1V, (**d**) M5V, and (**e**) AD Leo, an active M4.5V star. Wavelengths of peak photon flux and gases with significant absorption bands are indicated. surf avg, surface average; surf max, surface maximum.

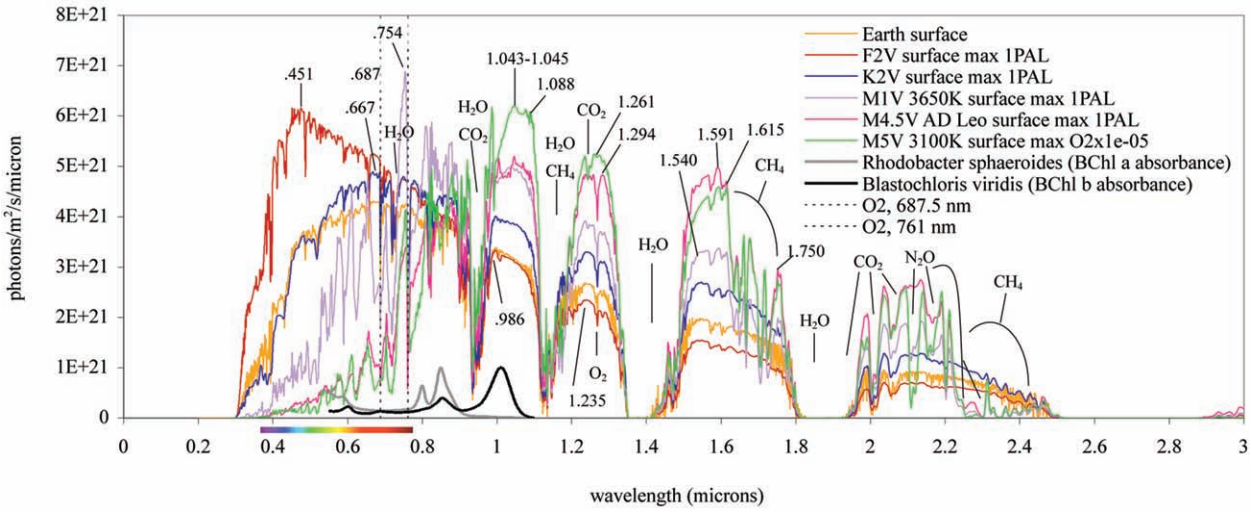

FIG. 3. Surface incident photon flux densities at solar noon for the Earth and for planets in the habitable zone of F, K, and M stars (temperatures of 3,650 K, 3,100 K, and measured AD Leo), as calculated from atmospheric composition in Segura *et al.* (2003, 2005) and the SMART radiative transfer model (Crisp, 1997). Wavelength of peak flux densities and transmittance window edges are indicated, as well as O_2 absorption lines. The absorbance spectra of bacteriochlorophyll (BChl) a and BChl b are included.

noon at the equator for these modeled scenarios: the F2V planet at 1 PAL; the Sun–Earth (K2V) at 1 PAL; M1V at 1 PAL; AD Leo at 1 PAL; and M5V at 10^{-5} O_2 PAL [source for the Sun–Earth same as Fig. 2 in Kiang *et al*. (2007)]. In addition, the locations of major gas absorption bands are indicated (O_3, H_2O, CO_2), and dashed lines are plotted for the O_2 A- and B-bands.

While the solar flux at the Earth's surface peaks in the red at about 685 nm, the peak for the F2V planet is in the violet at 451 nm. The K2V planet has its peak photon flux at 667 nm. The hottest M dwarf planet, M1V 3650K, peaks at 754 nm, within the red edge region. The M5V 3,100 K and AD Leo planets have their peak fluxes at about 1,045 nm, in the X transmittance window where bacteriochlorophyll b in *Blastochloris viridis* (formerly *Rhodopseudomonas viridis*) is able to absorb. The peaks would correspond to where extrasolar photosynthetic pigments would have their peak absorbance, according to our rule in section 2.2.1 for the influence of incident spectral photon fluxes. Minor peaks are also indicated in the other transmittance windows in Fig. 3. The wavelengths of peak PPFD are summarized in Table 2a. Table 2a also summarizes the integrated PAR-relevant fluxes in different transmittance windows, which we will discuss in more detail later.

Table 2b gives the time-averaged global PPFD. The average G2V surface PPFD in Table 2b is 3.2×10^{20} photons/m^2/s for clear sky conditions, compared to 3.1×10^{20} in Zhang *et al*. (2004). So, our estimates for the G2V planet appear fairly accurate [Wolstencroft and Raven (2002) estimated an absorbed 1.40×10^{21} photons/m^2/s for a cloudless G2V planet at the inner edge of the habitable zone].

Since photosynthesis on Earth developed first under water, and it is sedimentation of fixed carbon in the ocean that primarily drives the buildup of atmospheric oxygen, we are also interested in photon flux densities under water for when the atmosphere is low in oxygen. Figure 4a shows the maximum (at solar noon at the equator) spectral flux density at a depth of 5 cm of pure water for all the star types, with the F, K, and quiescent M1V and M5V planet atmospheres at negligible O_2 concentrations. This illustrates how water absorbance reduces the available NIR photons on all the planets. Figure 4b shows the maximum underwater spectral flux density at several depths for the M5V planet with no oxygenic photosynthesis. The lower photon flux limit is set at the level of the Black Sea and hydrothermal vent bacteria at 1.8×10^{15} photons/m^2/s (this is just an indicator, since the available photon flux would be integrated over a band). Underwater photon fluxes are strongly curtailed at wavelengths above 1.34 μm for a depth of 5 cm, or above 1.14 μm at depths 20 cm and deeper.

TABLE 2. SURFACE AND UNDERWATER INCIDENT PHOTON FLUX DENSITIES FOR CLOUDLESS PLANETS (a) AT SOLAR NOON AND (b) ILLUMINATED FACE AVERAGE

	Photon flux density ($\times 10^{20}$ photon/m^2/s)								
						M5V		*M5V Under water ($O_2 \times 10^{-5}$)*	
	F2V (1 PAL)	*G2V (Sun/Earth)*	*K2V (1 PAL)*	*M1V (1 PAL)*	*M4.5V (1 PAL)*	*($O_2 \times 10^{-5}$)*	*1 PAL*	*5 cm*	*100 cm*
a. Solar noon									
UVB 280–315 nm	0.049	0.018	0.015	0.001	0.000	0.000	0.000	—	—
UVA 315–400 nm	2.319	0.871	0.588	0.095	0.021	0.016	0.016	—	—
PAR									
400–700 nm	16.4	11.0	11.5	6.1	1.8	1.5	1.5	1.4	1.1
400–1,100 nm	29.8	23.8	26.3	23.2	16.1	17.3	16.9	9.9	1.5
400–1,400 nm	34.0	28.6	32.1	29.3	23.7	25.7	24.9	10.2	1.5
400–1,800 nm	37.9	33.7	38.9	36.4	34.2	35.3	34.3	10.2	1.5
400–2,500 nm	40.5	36.9	43.3	40.2	40.0	40.1	38.4	10.2	1.5
Peak photon flux	450.8	668.5	666.6	753.5	1,045.1	1,042.8	1,042.8	1,073.2	1,073.2
Wavelength range (nm)	451.0	685.5	667.8	754.3	1,045.9	1,043.6	1,043.6	1,075.7	1,075.7
b. Illuminated face average									
UVB 280–315 nm	0.006	0.017	0.003	0.000	0.000	0.000	0.000	—	—
UVA 315–400 nm	0.940	0.518	0.241	0.040	0.009	0.007	0.007	—	—
PAR									
400–700 nm	7.5	6.3	5.4	2.9	0.9	0.7	0.7	0.7	0.5
400–1,100 nm	13.8	12.4	12.3	10.8	7.4	7.8	7.8	4.7	0.7
400–1,400 nm	15.6	14.2	14.8	13.2	10.6	11.0	11.0	4.8	0.7
400–1,800 nm	17.4	16.4	17.9	16.2	15.0	15.0	15.0	4.8	0.7
400–2,500 nm	18.5	17.6	19.8	17.7	17.3	16.5	16.5	4.8	0.7

In b, average fluxes are approximated by the photon flux at a solar zenith angle of 60° from vertical.

6. DISCUSSION

6.1. Available PAR bands and pigment spectra

Several previous workers have addressed the various star type light limits for oxygenic photosynthesis (Heath *et al*., 1999; Franck *et al*., 2001; Wolstencroft and Raven, 2002; Cockell and Raven, 2004), so our numbers here provide more refined calculations for comparison of PPFDs. Wolstencroft and Raven (2002) estimated surface incident PPFD and PPFD at a 10-m ocean depth for planets around A0V, F0V, G0V, G2V, K0V, and M0V stars. Our modeled stars—F2V, G2V, M1V, M4.5V, and M5V—except for the M4.5V and M5 stars, are comparable to theirs. Wolstencroft and Raven (2002) assumed spectral peaks according to blackbody radiation, so here we provide the non-blackbody spectra for M stars as in Segura *et al*. (2003, 2005). With the SMART radiative transfer model (Meadows and Crisp, 1996; Crisp, 1997), we can now define spectral photon fluxes in line-by-line detail.

On these different stars, a few different radiation bands could be potentially photosynthetically active. For the F, G, and K stars, since there is abundant visible light, it is most likely that a visible 400–700 nm band would be the dominant PAR band. In contrast, for the M star planets, there is significantly higher PPFD in the NIR than in the visible compared to the planets around F, G, and K stars, with the available radiation occurring in distinct windows. So, it could be advantageous on such planets for PAR to extend to the NIR. If pigments evolve at the surface, then the PAR range could extend to 1,800 nm and possibly to 2,500 nm.

In the underwater spectra in Fig. 4, the 1.14 μm upper wavelength cutoff to the X band and the 1.34 μm cutoff for only very shallow organisms above 5 cm indicate it is unlikely that photosynthesis developing under water will evolve pigments that absorb above about 1.340 μm, and most likely the pigments will absorb somewhere below 1.140 μm, with the cutoff getting shorter with depth. All aquatic and marine photosynthesizers would be restricted to below this wavelength. Their land plant offspring may be confined to these bands, but it is also possible that

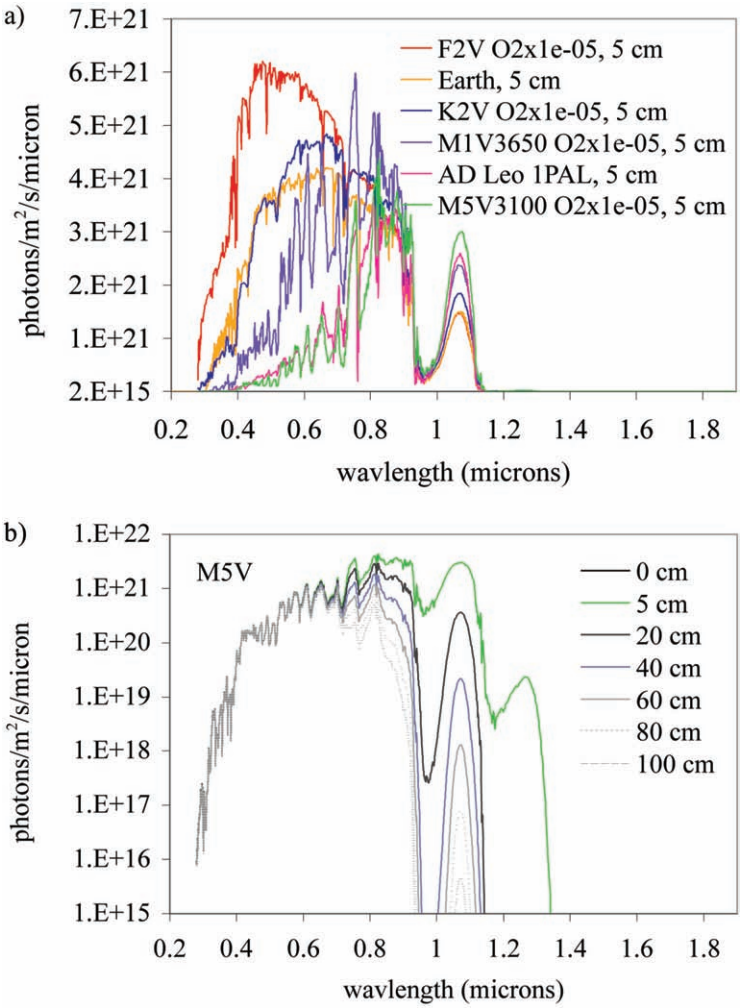

FIG. 4. Underwater planetary maximum photon flux densities for star–atmosphere scenarios in Table 2. (**a**) Photon fluxes at a depth of 5 cm in pure water. (**b**) Photon fluxes at the surface and several depths for an M5V 3,100 K star with negligible atmospheric O_2 (10^{-5} PAL).

pigments can evolve for new environments to absorb at wavelengths different from their ancestors.

So, for M star planets, PAR bands in the NIR could have the following restrictions: a 1.040 μm three-photosystem upper wavelength limit for the energy equivalent required by PS II and PS I, a 1.100 μm upper wavelength thermal limit, and transmittance windows where there is the most available radiation. We can allow for the possibility that an extrasolar photosynthesizer could achieve slightly better efficiency and fix carbon with a three-photosystem arrangement out to 1,100 nm. We, therefore, define extended PAR bands for M star planets. These bands correspond closely to the W, X, Y, Z, and Q windows defined in Fig. 2b, rounded to the nearest tenth of a micron; since the regions at the window cutoffs in the NIR are noisy and spread out, a higher precision makes little difference in the integrated photon flux. Also, since organisms absorbing at longer wavelengths will most likely also harvest light at the shorter wavelengths via resonance transfer, each PAR band includes the shorter-wavelength bands. The extended PAR bands are 0.4–1.1 μm, 0.4–1.4 μm, 0.4–1.8 μm, and 0.400–2.5 nm. These correspond to photosystems that utilize, respectively, 1.5 times, two times, three times, and four times as many photons per carbon fixed as Earth organisms.

For the F, G, and K star planets, the PAR band would most likely be just the same as on Earth, 0.4–0.7 μm, with limited photosynthesis at wavelengths up to 1.1 μm. The bounds of the shorter PAR band could be set at 0.400–0.730 μm to acknowledge the ability of *Acaryochloris marina* to utilize the longer wavelengths (Chen *et al.*, 2005), but for the sake of intercomparison with common numbers in the literature, we stick to the traditional 0.7 μm cutoff.

For all of the simulated stars/atmosphere combinations, the solar noon surface flux densities in

all bands in Table 2a are bright enough to sustain photosynthesis above the light compensation points for the Black Sea and hydrothermal vent bacteria at 1.8×10^{15} photons/m^2/s (Overmann *et al.*, 1992; Beatty *et al.*, 2005), and for green plants at 1.8×10^{18} photons/m^2/s (Nobel, 1999). The M star planets' photon fluxes in the 0.4–1.1 μm band are more than twice the Earth's visible PPFD. Therefore, even planets around M stars could ostensibly host land-based plants. Meanwhile, the K stars and quiescent M stars produce low UV well below the range experienced by Earth organisms, even without an ozone shield.

The presence of 1 PAL oxygen on the M5V 3,100 K planet does not significantly lower the integrated PPFD, but it causes very narrow band dips in PPFD at 0.687, 0.761, and 1.269 μm. Hence, though oxygen may demarcate PAR bands for photosynthetic pigments and slightly shift the visible spectrum, it does not greatly affect light availability compared to a planet with anoxygenic photosynthesis. The oxygen spectral influence would be more important for an M1V 3,650 K planet in the visible, whereas for the cooler M stars with little visible light, it would be more important at the 1.269 μm line.

So, spectrally we have some sense for the wavelengths at which reaction centers and pigments may peak in photon absorbance. The peak PPFD wavelengths summarized in Table 2a are not necessarily at the edges of their respective transmittance windows, so possibly there may be uphill and downhill excitation energy transfer, or the reaction center peaks may be shifted to the edges of the conjectured PAR bands, with accessory pigments harvesting in the rest of the band. The peak at 0.754 μm for the M1V star is in a region of the spectrum that is so variable that photons in longer NIR wavelengths may still be more reliable energy sources. In the NIR, the wavelength of peak PPFD at a 5 cm depth for the M5V planet is as for Earth, at water's peak transmittance at ~1.075 μm. Since the purple bacteria that are known to absorb at 1.020 μm (which is neither a peak flux nor a window edge wavelength) use that energy for uphill transfer to a reaction center at 0.960 μm (Trissl *et al.*, 1999), this could be the case on an extrasolar planet as well, and more work on the thermodynamics and kinetics of exciton transfer needs to be done to determine why 0.960 μm for the reaction center and 1.020 μm for the accessory pigment or some other wavelength could be an optimum. The wavelength limit may have to do with the energy cutoff between electronic transitions versus vibrational or thermal energy, as mentioned earlier.

6.2. *Productivity potential for multiple photosystems*

Having determined that our simulated planets meet minimum PPFD to support not only the most light-limited organisms found on Earth but also vascular plants at typical flux levels, we now look at the productivity potential at the global scale using the values in Table 2b, adjusting to average over time and account for clouds, as described earlier. The detectability of photosynthetic atmospheric signatures—oxygen and seasonal cycles of CO_2 and/or CH_4—will depend on the net global productivity of both ocean and land organisms. The detectability of surface spectra will depend on the photosynthesizers' cover and density over the planet. As the purpose of this study is to examine planets in the habitable zone (where liquid water exists), and resource constraints on another planet may be arbitrary, we can assume sufficient water and nutrients as a plausible case, and the extreme limits of photosynthesis are of concern primarily with respect to how much they will affect the spectral properties, productivity, and hence detectability of photosynthesis.

Table 3 summarizes the global time-averaged PPFDs and the O_2 or CO_2 flux from NPP, weighted for 26% ice-free land and 71% ocean for the planets around the other stars. The GPP values are given assuming the same quantum efficiency as on Earth, as well as using 1.5 times, two times, three times, and four times quantum requirements for the PAR bands that extend to the NIR. Also, since underwater photosynthesis will have more limited useful wavelengths, only the PAR 0.4–1.1 μm and 0.4–1.4 μm bands are used for the ocean. As a reference, Earth's GPP is given in bold (0.72×10^{18} quanta of $CO_2/m^2/s$ is equivalent to ~110 Pg-C/year, where quanta are molecules).

In the 0.4–1.1 μm PAR band, all of the stars cooler than the Sun have photon fluxes at the planetary surface well above the visible photon fluxes at the Earth's surface. If three-photosystem photosynthesis is used (1.5 times quantum requirement over 400–1,100 nm), then the M1V planet could still have a productivity above that of Earth's, but the other M stars would be only about 75% as productive as the Earth, at Earth-

Table 3. Global Time-Averaged Surface Incident Photon Flux Densities and Potential GPP for Planets with Oxygenic or Anoxygenic Photosynthesis, and for Cases of Photosystem Quantum Requirements That Are (1) Equal to That on Earth and (2) with Double, Triple, and Quadruple the Quantum Requirements, Respectively, for the 400–1,100, 400–1,400 nm, 400–1,800 nm, and 400–2,500 nm PAR Bands

	F2V (1 PAL)	*G2V (Sun/Earth)*	*K2V (1 PAL)*	*M1V (1 PAL)*	*M4.5V (1 PAL)*	*M5V*	
						($O_2 \times 10^{-5}$)	*1 PAL*
Time- and disk-averaged surface incident radiation ($\times 10^{20}$ photons/m^2/s)							
UVB 280–315 nm	0.002	0.006	0.001	0.000	0.000	0.000	0.000
UVA 315–400 nm	0.357	0.197	0.092	0.015	0.003	0.003	0.003
PAR							
400–700 nm	2.8	2.4	2.0	1.1	0.3	0.3	0.3
400–1,100 nm	5.2	4.7	4.7	4.1	2.8	3.0	3.0
400–1,400 nm	5.9	5.4	5.6	5.0	4.0	4.2	4.2
400–1,800 nm	6.6	6.2	6.8	6.2	5.7	5.7	5.7
400–2,500 nm	7.0	6.7	7.5	6.7	6.6	6.3	6.3
GPP with Earth-like quantum requirements ($\times 10^{18}$ quanta/m^2/s)							
PAR							
400–700 nm	0.85	**0.72**	0.61	0.33	0.10	0.08	0.08
400–1,100 nm	1.56	1.40	1.39	1.22	0.84	0.88	0.88
400–1,400 nm	1.76	1.60	1.68	1.50	1.20	1.25	1.25
400–1,800 nm	1.87	1.74	1.86	1.68	1.46	1.48	1.48
400–2,500 nm	1.94	1.81	1.97	1.76	1.59	1.57	1.57
GPP at 1.5×, 2×, 3×, and 4× quantum requirements ($\times 10^{18}$ quanta/m^2/s)							
PAR							
400–1,100 nm	1.04	—	0.93	0.81	0.56	0.59	0.59
400–1,400 nm	0.88	—	0.84	0.75	0.60	0.62	0.62
400–1,800 nm	0.62	—	0.62	0.56	0.49	0.49	0.49
400–2,500 nm	0.48	—	0.49	0.44	0.40	0.39	0.39

like efficiencies and the given land/ocean coverage. If a four-photosystem series is used (two times quantum requirement over 0.4–1.4 μm), the M1V planet can still maintain a productivity close to that of Earth's, while the M4.5V and M5V planets increase slightly to 80% of Earth's productivity. If triple or quadruple quantum requirements are necessary, then productivity on the M4.5V and M5V planets would drop to two-thirds to a half that of Earth. Multiple photosystems with graduated quantum requirements with each extension of the PAR bands to the NIR could boost the productivity, but the M4.5V and M5V planets would still be below Earth's productivity if utilizing only the 0.4–1.4 μm band; the longer bands would actually almost provide the necessary quantum flux, but also require that pigments evolve outside the water. Productivity will be limited by the availability of S, Fe, and H_2 (estimated for the early anoxic Earth by Canfield *et al*., 2006). On planets like Venus and Mars, sulfur is quite abundant (Schulze-Makuch *et al*., 2004; Wang *et al*., 2006) and may not be too limiting, but its utilization outside of marine or aquatic environments would require the ingenuity of an extrasolar photosynthesizer.

How the lower productivities might affect the atmospheric signature of oxygenic photosynthesis depends on the redox chemistry and history of the planet for the buildup of oxygen. Catling *et al*. (2005) reviewed the parameters that affect the oxygenation time: planetary size, which affects tectonic activity and hydrogen escape; the presence of continents, which affects weathering, oceanic heat flux, and carbon burial; planet composition, which determines whether conditions are more oxidizing or reducing; and the community composition of the biosphere, which affects cycling and burial of organic and inorganic carbon. Although we simulate planets with the same size as and similar continental fraction as the Earth, we cannot simulate full biogeochemical cycles to predict the buildup of atmospheric O_2, but we make comparisons, assuming otherwise Earth-like ratios of sources and sinks of O_2. On Earth, about 0.1 Pg-C/year is buried in ocean sediments, or about 0.2% of ocean NPP. In the simulations in Segura *et al*. (2003) of the atmospheres of planets around F2V, G2V, and K2V stars, O_2 is observable in the visible for atmospheres with at least 10^{-2} PAL O_2, and O_3 can be observed in the thermal-infrared in atmospheres with at least

10^{-3} PAL O_2. So, if the level of productivity is linearly related to the concentration of atmospheric O_2, then the dim M5V planets could still show a strong enough biosignature.

Other scenarios of land/ocean configurations can be conceived, with land concentrated at the equator versus the poles, variations in efficiencies of light use, etc. The oceans and land compete, however, for the strength of biosignatures. Increasing the size of the oceans could enhance the O_2 signature but then weaken the land surface signature. Although algal blooms can create a strong signature for satellite detection (Carder and Steward, 1985; Lubin *et al*., 2001), their extent at the global scale is too sparse for detection in a disk-average spectrum (Tinetti *et al*., 2006b). Meanwhile, the location of land toward the poles or equator, or between hemispheres, as well as land productivity would determine the strength of a seasonal signal, if any. It may be difficult to discern a seasonal-type atmospheric biosignature for M4.5V–M5V planets that utilize only visible PAR for photosynthesis.

6.3. UV flares and photosynthesis under water

Because UV flares during the early life of M stars may push organisms to deeper water for protection, there may be a conflict between UV screening versus availability of PAR [Raven and Wolstencroft (2004) called this "feast or famine"]. Here we estimate the depths of water at which organisms would be safe from flares of different magnitudes, assuming that they have no UV screening pigments. UV damage to plants has been observed at doses of 15–16 kJ/day (Kakani *et al*., 2003). The spectral quality of M star flares is not well known, but they may span the X-ray, UV, and visible. Segura *et al*. (2005) summarized their magnitudes and duration, and some flares from AD Leo. Flares may be as small as $\sim 10^{28}$ ergs of radiative energy and occur fairly frequently ($\sim$0.71/h) (Crespo-Chacon *et al*., 2006); the largest observed are 10^{34}–10^{37} ergs, and the flares larger than $\sim 10^{32}$ ergs occur at a rate of roughly one per day on very active stars. On AD Leo, flares on the order of 10^{32} ergs occur approximately every 4 days, and a flare of size 7.1×10^{32} ergs was observed to have 70% of its energy in the UV at 0.200–0.326 μm (Hawley and Pettersen, 1991).

To estimate the strongest dose that organisms could receive at the surface of a planet, we looked at the doses for a planet around AD Leo, whose extremely high activity represents a possible upper limit to UV emissions (Segura *et al*., 1993). Although damage from UV is more precisely estimated with action spectra for DNA damage, since these action spectra as well as flare spectra are so variable, we used integrated estimates of the 15 kJ/day plant dose and the average water absorbance of radiation over 0.200–0.326 μm from the spectrum of Segelstein (1981) (weighted by photon energy, this gives an absorbance of $\sim$0.01 cm^{-1}). Given the above occurrence rates of the flares and the semimajor axis of 0.16 AU from AD Leo, we solved for the safe depths from UV damage, at which the available UV from the flare is less than the minimum plant dose. Table 4 summarizes these depths, as well as the visible

Table 4. Water Depths Safe from UV Flares: Available Visible (0.4–0.7 μm) and NIR (0.7–1.1 μm) for AD Leo

Flare frequency (d^{-1})	*Flare size (ergs)*	*Safe depth (m)*	*photons/m² × 10²⁰ for M4.5V AD Leo*	
			Visible	*NIR*
17	1.0×10^{28}	0.0	0.9	6.6
17	1.0×10^{29}	0.0	0.9	6.6
17	1.0×10^{30}	0.0	0.9	6.6
17	1.0×10^{31}	0.0	0.9	6.6
1	1.0×10^{32}	0.0	0.9	6.6
1	1.0×10^{33}	0.0	0.9	6.6
1	1.1×10^{33}	0.05	0.8	3.7
1	5.0×10^{33}	1.5	0.61	0.1
1	1.0×10^{34}	2.2	0.5	3×10^{-2}
1	1.0×10^{35}	4.5	0.3	3×10^{-3}
1	1.0×10^{36}	6.8	0.3	6×10^{-4}
1	1.0×10^{37}	9.1	0.2	1×10^{-4}

(0.4–0.7 μm) and NIR (0.7–1.1 μm) PAR photon flux density averages for the illuminated face of a rotating planet.

The smaller flares of 10^{28}–10^{31} ergs, even at their higher rate of occurrence, do not produce enough UV to be damaging even outside of the water. Also, the flares of order 10^{32} ergs, even at a higher rate than on AD Leo, produce below the plant damage limit at the surface. The flares of $\sim 10^{33}$ ergs are at the threshold at which protection under water is necessary. The largest flares of 10^{37} ergs result in dangerous UV doses down to at least a water depth of 9.1 m. However, even at this depth, AD Leo provides visible radiation an order of magnitude above the lower limit of 1.8×10^{18} photons m^{-2} s^{-1} for green plants (Nobel, 1999), and well above the red algae limit of 6×10^{15} photons m^{-2} s^{-1} (Overmann *et al*., 1992). Although the NIR drops off significantly with depth, its photon flux at the 9.1 m water depth is still above the red algae limit; also, organisms at this depth would harvest the visible as well as NIR photons. Therefore, photosynthetic organisms during the flaring stage of M star planets should be able to survive even with visible light, though their productivity would be limited to less than 14% of Earth's with smaller flares and less than 4% with very active M stars like AD Leo with daily large flares.

7. CONCLUSIONS

From Earth's example, we have proposed how photosynthesis is likely to evolve with a different parent star and atmospheric chemistry, and produce predictable alternative pigment spectra and atmospheric signatures. We do not know enough yet to predict full reflectance spectra.

During our survey of Earth-based photosynthetic organisms, we observed that a number of molecular-scale chemical constraints and global scale environmental pressures determine the optimum wavelength of peak absorbance of PAR (Kiang *et al*., 2007). Photosynthetic pigments on extrasolar planets are likely to evolve to peak in absorbance at the wavelengths at which the transmitted light at the planet's surface is highest in photon flux densities or most energetic for transfer to longer-wavelength reaction centers. Oxygenic photosynthesis could be possible over wavelengths up to even beyond 2.5 μm, given a sufficient number of photosystems chained together and barring a longer wavelength limit for vibrational versus electronic energy transitions. However, pigments that evolve under water are unlikely to absorb above 1.4 nm or even 1.1 nm. Anoxygenic photosynthesis would have the same PAR band restrictions. Planets around F2V stars might have a "blue edge" or at least be darker in the blue. K2V planets would look very similar to the Earth. The M stars could have several different PAR bands: they might have multiple critical absorption wavelengths in the visible, because of their noisy spectra in this region; and the dominant photosynthetic organisms would most likely harvest light over 0.4–1.1 μm, with potential but unlikely extensions to 1.4 and 2.5 μm.

All of the star–planet combinations we simulated have more than sufficient light to support Earth-like photosynthesis. The low productivity of the M4.5V and M5V planets, if oxygenic, could be sufficient to produce observable oxygen, but probably take longer to do so. Redox energetics imply that longer-wavelength photons could be used in chains of several linked photosystems to provide enough energy to abstract electrons and fix CO_2.

For the purpose of observing terrestrial extrasolar planets, we cannot yet determine how strong the red edge contrast will likely be for detection purposes, and given the example of lichens, there might not be a distinct edge. Remote sensing studies indicate that lichens can be distinguished from the mineral background (Ager and Milton, 1987; Rees *et al*., 2004), so global-scale modeling like that of Tinetti *et al*. (2006b,c) will help us to determine how detectable a lichen-like signature might be.

This investigation of the light spectrum at the surface of planets around other star types offers the next refinement in quantifying the nature of photosynthesis on extrasolar planets, particularly around M stars. Here we focused on predicting and identifying photosynthetic biosignatures through narrowing the possibilities for pigment absorbance spectra. We have identified where deeper understanding of photosystem energetics is needed to restrict potential pigment absorbance wavelengths. Because more data are needed to explain the apparent variation in the NIR reflectance spectra across organism functional types, particularly algae and bacteria, we have *not* attempted to simulate a full surface reflectance spectrum and its detectability in the radiance spectrum of the planet. More studies are needed

to assess the likelihood of, for example, the edge-like reflectance feature of the hypothetical NIR-shifted reflectance spectrum that Tinetti *et al*. (2006c) simulated for photosynthesis around M stars.

Additional modeling investigations that are called for include the following: three-dimensional modeling to refine calculations of photosynthetic productivity by climate zones and as affected by cloud cover; more three-dimensional radiative transfer modeling to detect alternative pigments and whole-canopy reflectance spectra; and coupled biogeochemical/atmosphere models to quantify net fluxes to the atmosphere and the possible amplitude in temporal variation. For instrument design, modeling is needed to determine the spectral resolution necessary to resolve a pigment feature in a time- and disk-averaged radiance spectrum of the planet [*e.g*., Tinetti *et al*. (2006c) examined the red edge detectability on Earth]. Future work is also needed to assess an optimum resolution to capture pigment spectra that could be as sharp as that of terrestrial plants or as gradual as those of lichens or purple bacteria. If photosynthesis occurs in sulfur-rich clouds as on Venus, then even more complex modeling of cloud spectral radiative transfer would be another challenge. Finally, a survey should be conducted of mineral types to distinguish extrasolar photosynthetic signatures from the mineral surface.

Biosignatures—both atmospheric and surface—on planets around M stars may actually be easier to detect than those around F, G, or K stars. The modeled atmospheres of M star planets of Segura *et al*. (2005) reveal that low UV radiation from quiescent M stars could result in higher concentrations of biogenic gases CH_4, N_2O, and CH_3Cl. Tinetti *et al*. (2006b,c) found the "red edge," shifted to the NIR, to be easier to detect through modeled clouds than the plant red edge. These prospects to detect life should motivate continued investigations into M star atmospheres and the spectral adaptations of extrasolar photosynthesis.

8. ACKNOWLEDGMENTS

We are greatly obliged to Niels-Ulrik Frigaard, Richard Cogdell, and Andrew Gall for pigment data and valuable comments; Brian Cairns, Judith Lean, and Andrew Lacis for solar spectral photon flux densities for the Earth; and David Mauzerall, Warwick Hillier, Yongqin Jiao, and Elmars Krausz for very helpful explanations about photochemistry. We also thank John Scalo, Norm Sleep, and Jim Kasting for many lively discussions and helpful references. Thanks are due to two anonymous reviewers who helped greatly to improve this paper. This work was performed as part of the NASA Astrobiology Institute's Virtual Planetary Laboratory Lead Team effort, supported under NASA Cooperative Agreement Number CAN-00–OSS-01. M.C. thanks NASA for supporting his participation in this work through Jet Propulsion Laboratory contract number 1234394 with the University of California, Berkeley. Govindjee thanks the Department of Plant Biology of the University of Illinois for office support. N.Y.K also thanks NASA and James Hansen for supporting this work.

9. ABBREVIATIONS

GPP, gross primary productivity; NIR, near-infrared; NO_x, nitric oxides; NPP, net primary productivity; PAL, present atmospheric level; PAR, photosynthetically active radiation; Pg, petagrams; PPFD, photosynthetic photon flux density; PS I, Photosystem I; PS II, Photosystem II; UV, ultraviolet.

10. REFERENCES

Ager, C.M. and Milton, N.M. (1987) Spectral reflectance of lichens and their effects on the reflectance of rock substrates. *Geophysics* 52(7), 898–906.

Arnold, L., Gillet, S., Lardiere, O., Riaud, P., and Schneider, J. (2002) A test for the search for life on extrasolar planets: looking for the terrestrial vegetation signature in the Earthshine spectrum. *Astron. Astrophys*. 392(1), 231–237.

Basri, G., Borucki, W.J., and Koch, D. (2005) The Kepler Mission: a wide-field transit search for terrestrial planets. *New Astron. Rev*. 49(7–9), 478–485.

Beatty, J.T., Overmann, J., Lince, M.T., Manske, A.K., Lang, A.S., Blankenship, R.E., Van Dover, C.L., Martinson, T.A., and Plumley, F.G. (2005) An obligately photosynthetic bacterial anaerobe from a deep-sea hydrothermal vent. *Proc. Natl. Acad. Sci. U S A* 102(26), 9306–9310.

Beaulieu, J.-P., Bennett, D.P., Fouque, P., Williams, A., Dominik, M., Jorgensen, U.G., *et al*. (2006) Discovery of a cool planet of 5.5 Earth masses through gravitational microlensing. *Nature* 439(7075), 437–440.

Beichman, C.A., Woolf, N.J., and Lindensmith, C.A. (1999) *The Terrestrial Planet Finder (TPF): A NASA Origins Program to Search for Habitable Planets*, JPL Publication No. 99–003, NASA Jet Propulsion Laboratory, Pasadena, CA.

Blankenship, R.E. (2002) *Molecular Mechanisms of Photosynthesis*, Blackwell Science, Oxford, UK.

Bordé, P., Rouan, D., and Léger, A. (2003) Exoplanet detection capability of the COROT space mission. *Astron. Astrophys*. 405(3), 1137–1144.

Borucki, W.J., Koch, D.G., Basr, G.B., Caldwell, D.A., Caldwell, J.F., Cochran, W.D., DeVore, E., Dunham, E.W., Geary, J.C., Gilliland, R.L., Gould, A., Jenkins, J.M., Kondo, Y., Latham, D.W., and Lissauer, J.J. (2003) The Kepler Mission: finding the sizes, orbits, and frequencies of Earth-size and larger extrasolar planets. In *ASP Conference Series, Vol. 294: Scientific Frontiers in Research on Extrasolar Planets*, edited by D. Deming and S. Seager, Astronomical Society of the Pacific, San Francisco, pp. 427–440.

Butler, R.P., Vogt, S.S., Marcy, G.W., Fischer, D.A., Wright, J.T., Henry, G.W., Laughlin, G., and Lissauer, J.J. (2004) A Neptune-mass planet orbiting the nearby M dwarf GJ 436. *Astrophys. J.* 617(1), 580–588.

Campbell, B.J., Jeanthon, C., Kostka, J.E., Luther, G.W.I., and Cary, S.C. (2001) Growth and phylogenetic properties of novel bacteria belonging to the epsilon subdivision of the Proteobacteria enriched from *Alvinella pompejana* and deep-sea hydrothermal vents. *Appl. Environ. Microbiol*. 67(10), 4566–4572.

Canfield, D.E., Rosing, M.T., and Bjerrum, C. (2006) Early anaerobic metabolisms. *Philos. Trans. R. Soc. B Biol. Sci*. 361(1474), 1819–1834.

Carder, K.L. and Steward, R.G. (1985) A remote-sensing reflectance model of a red-tide dinoflagellate off west Florida. *Limnol. Oceanogr*. 30(2), 286–298.

Catling, D.C., Zahnle, K.J., and McKay, C.P. (2001) Biogenic methane, hydrogen escape, and the irreversible oxidation of early Earth. *Science* 293(5531), 839–843.

Catling, D.C., Glein, C.R., Zahnle, K.J., and McKay, C.P. (2005) Why O_2 is required by complex life on habitable planets and the concept of planetary "oxygenation time." *Astrobiology* 5(3), 415–438.

Chen, M., Telfer, A., Lin, S., Pascal, A., Larkum, A.W.D., Barber, J., and Blankenship, R.E. (2005) The nature of the photosystem II reaction centre in the chlorophyll d-containing prokaryote, *Acaryochloris marina. Photochem. Photobiol. Sci*. 4(12), 1060–1064.

Cockell, C.S. and Raven, J.A. (2004) Zones of photosynthetic potential on Mars and the early Earth. *Icarus* 169(2), 300–310.

Cramer, W., Kicklighter, D.W., Bondeau, A., Moore, B.I., Churkina, G., Nemry, B., Ruimy, A., and Schloss, A.L. (1999) Comparing global models of terrestrial net primary productivity (NPP): overview and key results. *Global Change Biol*. 5(Suppl. 1), 1–15.

Crespo-Chacon, I., Montes, D., Garcia-Alvarez, D., Fernandez-Figueroa, M., Lopez-Santiago, J., and Foing, B. (2006) Analysis and modeling of high temporal resolution spectroscopic observations of flares on AD Leonis. *Astron. Astrophys*. 452(3), 987–1000.

Crisp, D. (1997) Absorption of sunlight by water vapor in cloudy conditions: a partial explanation for the cloud absorption anomaly. *Geophys. Res. Lett*. 24(5), 571–574.

Ferreira, K.N., Iverson, T.M., Maghlaoui, K., Barber, J., and Iwata, S. (2004) Architecture of the photosynthetic oxygen-evolving complex. *Science* 303(5665), 1831–1838.

Franck, S., von Bloh, W., Bounama, C., Steffen, M., Schönberner, D., and Schellnhuber, H.-J. (2001) Limits of photosynthesis in extrasolar planetary systems for Earth-like planets. *Adv. Space Res*. 28(4), 695–700.

Gould, A., Udalski, A., An, D., Bennett, D.P., Zhou, A.-Y., Dong, S., Rattenbury, N.J., Gaudi, B.S., Yock, P.C.M., Bond, I.A., Christie, G.W., Horne, K., Anderson, J., Stanek, K.Z., DePoy, D.L., Han, C., McCormick, J., Park, B.-G., Pogge, R.W., Poindexter, S.D., Soszynski, I., Szymanski, M.K., Kubiak, M., Pietrzynski, G., Szewczyk, O., Wyrzykowski, L., Ulaczyk, K., Paczynski, B., Bramich, D.M., Snodgrass, C., Steele, I.A., Burgdorf, M.J., Bode, M.F., Botzler, C.S., Mao, S., and Swaving, S.C. (2006) Microlens OGLE-2005-BLG-169 implies cool Neptune-like planets are common. *Astrophys. J*. 644(1), L37–L40.

Govindjee (1999) On the requirement of minimum number of four versus eight quanta of light for the evolution of one molecule of oxygen in photosynthesis: a historical note. *Photosynthesis Res*. 59(2–3), 249–254.

Grace, J. and Rayment, M. (2000) Respiration in the balance. *Nature* 404(6780), 819–820.

Grant, L. (1987) Diffuse and specular characteristics of leaf reflectance. *Remote Sensing Environ*. 22(2), 309–322.

Grinspoon, D.H. (1997) *Venus Revealed: A New Look Below the Clouds of Our Mysterious Twin Planet*, Perseus Publishing, Cambridge, MA.

Guenther, A., Hewitt, C.N., Erickson, D., Fall, R., Geron, C., Graedel, T., Harley, P., Klinger, L., Lerdau, M., McKay, W.A., Pierce, T., Scholes, B., Steinbrecher, R., Tallamraju, R., Taylor, J., and Zimmerman, P. (1995) A global model of natural volatile organic compound emissions. *J. Geophys. Res*. 100(D5), 8873–8892.

Hart, M.H. (1978) The evolution of the atmosphere of the Earth. *Icarus* 33(1), 23–39.

Hawley, S.L. and Pettersen, B.R. (1991) The great flare of 1985 April 12 on AD Leonis. *Astrophys. J*. 378(2), 725–741.

Heath, M.J., Doyle, L.R., Joshi, M.M., and Haberle, R.M. (1999) Habitability of planets around red dwarf stars. *Orig. Life Evol. Biosph*. 29, 405–424.

Hill, R. and Bendall, F.L. (1960) Function of the two cytochrome components in chloroplasts: a working hypothesis. *Nature* 186(4719), 136–137.

Hill, R. and Rich, P.R. (1983) A physical interpretation for the natural photosynthetic process. *Proc. Natl. Acad. Sci. U S A* 80(4), 978–982.

Ito, A. and Oikawa, T. (2004) Global mapping of terrestrial primary productivity and light-use efficiency with a process-based model. In *Global Environmental Change in the Ocean and on Land*, edited by M. Shiyomi, H. Kawahata, H. Koizumi, A. Tsuda, and Y. Awaya, TERRAPUB, Tokyo, pp. 343–358.

Joshi, M.M., Haberle, R.M., and Reynolds, R.T. (1997) Simulations of the atmospheres of synchronously rotating

terrestrial planets orbiting M dwarfs: conditions for atmospheric collapse and the implications for habitability. *Icarus* 129(2), 450–465.

Kakani, V.G., Reddy, K.R., Zhao, D., and Sailaja, K. (2003) Field crop responses to ultraviolet-B radiation: a review. *Agric. Forest Meteorol*. 120(1–4), 191–218.

Karl, D.M., Wirsen, C.O., and Jannasch, H.W. (1980) Deep-sea primary production at the Galapagos hydrothermal vents. *Science* 207(4437), 1345–1347.

Kasting, J.F. (2001) Earth history–The rise of atmospheric oxygen. *Science* 293(5531), 819–843.

Kasting, J.F., Whitmire, D.P., and Reynolds, R.T. (1993) Habitable zones around main sequence stars. *Icarus* 101(1–3), 108–128.

Kesselmeier, J. and Staudt, M. (1999) Biogenic volatile organic compounds (VOC): an overview of emission, physiology and ecology. *J. Atmos. Chem*. 33(1), 23–88.

Kiang, N.Y., Siefert, J., Govindjee, and Blankenship, R.E. (2007) Spectral signatures of photosynthesis. I. Review of Earth organisms. *Astrobiology* 7(1), 222–251.

Kou, L., Labrie, D., and Chylek, P. (1993) Refractive indices of water and ice in the 0.65–2.5μm spectral range. *Appl. Opt*. 32(19), 3531–3540.

Krishtalik, L.I. (1986) Energetics of multielectron reactions. Photosynthetic oxygen evolution. *Biochim. Biophys. Acta* 849(1), 162–171.

Krishtalik, L.I. (2003) pH-dependent redox potential: how to use it correctly in the activation energy analysis. *Biochim. Biophys. Acta* 1604(1), 13–21.

Lawson, P.R., Unwin, S.C., and Beichman, C.A. (2004) *Precursor Science for the Terrestrial Planet Finder*, Jet Propulsion Laboratory Publication No. 04–014, National Aeronautics and Space Administration and California Institute of Technology, Pasadena, CA.

Lean, J. and Rind, D. (1998) Climate forcing by changing solar radiation. *J. Clim*. 11(2), 3069–3094.

Leger, A. (2000) Strategies for remote detection of life: Darwin-IRSI and TPF missions. *Adv. Space Res.* 25(11), 2209–2223.

Leger, A., Pirre, M., and Marceau, F.J. (1993) Search for primitive life on a distance planet–relevance of O_2-detection and O_3-detection. *Astron. Astrophys*. 277(1), 309–313.

Leger, A., Ollivier, M., Altwegg, K., and Woolf, N.J. (1999) Is the presence of H_2O and O_3 in an exoplanet a reliable signature of a biological activity? *Astron. Astrophys*. 341(1), 304–311.

Lin, L.-H., Wang, P.-L., Rumble, D., Lippmann-Pipke, J., Boice, E., Pratt, L.M., Lollar, B.S., Brodie, E.L., Hazen, T.C., Andersen, G.L., DeSantis, T.Z., Moser, D.P., Kershaw, D., and Onstott, T.C. (2006) Long-term sustainability of a high-energy, low-diversity crustal biome. *Science* 314(5798), 479–483.

Lovelock, J.E. (1965) A physical basis for life detection experiments. *Nature* 207(4997), 568–570.

Lubin, D., Li, W., Dustan, P., Mazel, C.H., and Stamnes, K. (2001) Spectral signatures of coral reefs: features from space. *Remote Sensing Environ*. 75(1), 127–137.

McArthur, B.E., Endl, M., Cochran, W.D., Benedict, G.F., Fischer, D.A., Marcy, G.W., Butler, R.P., Naef, D., Mayor, M., Queloz, D., Udry, S., and Harrison, T.E. (2004) Detection of a Neptune-mass planet in the rho(1) Cancri system using the Hobby-Eberly telescope. *Astrophys. J*. 614(1), L81–L84.

McEvoy, J.P., Gascon, J.A., Batista, V.S., and Brudvig, G.W. (2005) The mechanism of photosynthetic water splitting. *Photochem. Photobiol. Soc*. 4(12), 940–949.

Meadows, V.S. and Crisp, D. (1996) Ground-based near-infrared observations of the Venus nightside: the thermal structure and water abundance near the surface. *J. Geophys. Res*. 101(E2), 4595–4622.

Montañes-Rodriguez, P., Palle, E., Goode, P.R., Hickey, J., Qiu, J., Yurchyshyn, V., Chu, M.C., Kolbe, E., Brown, C.T., and Koonin, S.E. (2004) The earthshine spectrum. *Adv. Space Res*. 34(2), 293–296.

Montañes-Rodriguez, P., Palle, E., Goode, P.R., Hickey, J., and Koonin, S.E. (2005) Globally integrated measurements of the Earth's visible spectral albedo. *Astrophys. J*. 629(2), 1175–1182.

Nobel, P.S. (1999) *Physicochemical and Environmental Plant Physiology*, Academic Press, San Diego, CA.

Olson, J.M. (2006) Photosynthesis in the Archean era. *Photosynthesis Res.* 99(2), 109–117.

Overmann, J., Cypionka, H., and Pfennig, N. (1992) An extremely low-light-adapted phototrophic sulfur bacterium from the Black Sea. *Limnol. Oceanogr*. 37(1), 150–155.

Parson, W.W. (1978) Thermodynamics of the primary reactions of photosynthesis. *Photochem. Photobiol*. 28(3), 389–393.

Pavlov, A.A. and Kasting, J.F. (2002) Mass-independent fractionation of sulfur isotopes in Archean sediments: strong evidence for an anoxic Archean atmosphere. *Astrobiology* 2(1), 27–41.

Pavlov, A.A., Kasting, J.F., Brown, L.L., Rages, K.A., and Freedman, R. (2000) Greenhouse warming by CH_4 in the atmosphere of early Earth. *J. Geophys. Res*. 105(E5), 11981–11990.

Raich, J.W. and Schlesinger, W.H. (1992) The global carbon dioxide flux in soil respiration and its relationship to vegetation and climate. *Tellus* 4B(2), 81–99.

Raven, J.A. and Wolstencroft, R.D. (2004) Constraints on photosynthesis on Earth and Earth-like planets. In *Proceedings of IAU Symposium 213*: *Bioastronomy 2002: Life Among the Stars*, edited by R.P. Norris and F.H. Stootman, Astronomical Society of the Pacific, San Francisco, pp. 305–308.

Rees, W.G., Tutubalina, O.V., and Golubeva, E.I. (2004) Reflectance spectra of subarctic lichens between 400 and 2400 nm. *Remote Sensing Environ*. 90(3), 281–292.

Rivera, E.J., Lissauer, J., Butler, R.P., Marcy, G.W., Vogt, S.S., Fischer, D.A., Brown, T., and Laughlin, G. (2005) A 7.5 Earth-mass planet orbiting the nearby star, GJ 876. *Astrophys. J*. 634(1), 625–640.

Rutherford, A.W. and Boussac, A. (2004) Water photolysis in biology. *Science* 303(5665), 1782–1784.

Sagan, C. (1961) The Planet Venus—recent observations shed light on the atmosphere, surface, and possible biology of the nearest planet. *Science* 133(3456), 849–858.

Schlesinger, W.H. (1997) *Biogeochemistry: An Analysis of Global Change*, Academic Press, San Diego.

Schulze-Makuch, D., Irwin, L.N., and Irwin, T. (2002) Astrobiological relevance and feasibility of a sample collection mission to the atmosphere of Venus. In *ESA SP-518: Second European Workshop on Exo-Astrobiology*, edited by H. Sawaya-Lacoste, ESA Publications Division, Noordwijk, The Netherlands, pp. 247–252.

Schulze-Makuch, D., Grinspoon, D.H., Abbas, O., Irwin, L.N., and Bullock, M.A. (2004) A sulfur-based survival strategy for putative phototrophic life in the venusian atmosphere. *Astrobiology* 4(1), 11–18.

Seager, S., Turner, E.L., Schafer, J., and Ford, E.B. (2005) Vegetation's red edge: a possible spectroscopic biosignature of extraterrestrial plants. *Astrobiology* 5(3), 372–390.

Segelstein, D.J. (1981) The complex refractive index of water [M.S. thesis], University of Missouri–Kansas City, Kansas City, MO.

Segura, A., Krelove, K., Kasting, J.F., Sommerlatt, D., Meadows, V., Crisp, D., Cohen, M., and Mlawer, E. (2003) Ozone concentrations and ultraviolet fluxes on Earth-like planets around other stars. *Astrobiology* 3(4), 689–708.

Segura, A., Kasting, J.F., Meadows, V., Cohen, M., Scalo, J., Crisp, D., Butler, R.A.H., and Tinetti, G. (2005) Biosignatures from Earth-like planets around M dwarfs. *Astrobiology* 5(6), 706–725.

Sleep, N.H. (2001) Biogeochemistry–Oxygenating the atmosphere. *Nature* 410(6826), 317–319.

Sogandares, F.M. and Fry, E.S. (1997) Absorption spectrum (340–640nm) of pure water. I. Photothermal measurements. *Appl. Opt*. 36, 8699–8709.

Tinetti, G., Meadows, V.S., Crisp, D., Fong, W., Fishbein, E., Turnbull, M., and Bibring, J.P. (2006a) Detectability of planetary characteristics in disk-averaged spectra. I: The Earth model. *Astrobiology* 6(1), 34–47.

Tinetti, G., Meadows, V.S., Crisp, D., Kiang, N.Y., Kahn, B., Velusamy, T., Bosc, E., and Turnbull, M. (2006b) Detectability of planetary characteristics in disk-averaged spectra. II. Synthetic spectra and light curves of the Earth. *Astrobiology* 6(6), 881–900.

Tinetti, G., Rashby, S., and Yung, Y.L. (2006c) Detectability of red-edge shifted vegetation on M-star terrestrial planets. *Astrophys. J. Lett*. 644(2), L129–L132.

Tommos, C. and Babcock, G.T. (2000) Proton and hydrogen currents in photosynthetic water oxidation. *Biochim. Biophys. Acta* 1458(1), 199–219.

Trissl, H.-W., Law, C.J., and Cogdell, R.J. (1999) Uphill energy transfer in LH2-containing purple bacteria at room temperature. *Biochim. Biophys. Acta* 1412(2), 149–172.

Tucker, C.J. (1976) Sensor design for monitoring vegetation canopies. *Photogram. Eng. Remote Sensing* 42(11), 1399–1410.

Wang, A., Haskin, L.A., Squyres, S.W., Jolliff, B.L., Crumpler, L., Gellert, R., Schroder, C., Herkenhoff, K., Hurowitz, J., Tosca, N.J., Farrand, W.H., Anderson, R., and Knudson, A.T. (2006) Sulfate deposition in subsurface regolith in Gusev Crater, Mars. *J. Geophys. Res. Planets* 111, E02S17, doi:10.1029/2005JE002513.

Watts, S.F. (2000) The mass budgets of carbonyl sulfide, dimethyl sulfide, carbon disulfide and hydrogen sulfide. *Atmos. Environ*. 34(5), 761–779.

Wayne, R.P. (1991) *Chemistry of Atmospheres*, Oxford University Press, Oxford, UK.

Wolstencroft, R.D. and Raven, J.A. (2002) Photosynthesis: likelihood of occurrence and possibility of detection on Earth-like planets. *Icarus* 157(2), 535–548.

Woolf, N.J., Smith, P.S., Traub, W.A., and Jucks, K.W. (2002) The spectrum of earthshine: a pale blue dot observed from the ground. *Astrophys. J*. 574(1), 430–433.

Woyke, T., Teeling, H., Ivanova, N.N., Hunteman, M., Richter, M., Gloeckner, F.O., Boffelli, D., Anderson, I.J., Barry, K.W., Shapiro, H.J., Szeto, E., Kyrpides, N.C., Mussmann, M., Amann, R., Bergin, C., Ruehland, C., Rubin, E.M., and Dubilier, N. (2006) Symbiosis insights through metagenomic analysis of a microbial consortium. *Nature* doi:10.1038/nature05192.

Wydrzynski, T.J. and Satoh, K., eds. (2005) *Advances in Photosynthesis and Respiration Series, Vol. 22: Photosystem II: The Light-Driven Water: Plastoquinone Oxidoreductase*, Springer, Dordrecht, The Netherlands.

Zhang, Y.C., Rossow, W.B., Lacis, A.A., Oinas, V., and Mischenko, M.I. (2004) Calculation of radiative fluxes from the surface to top of atmosphere based on ISCCP and other global data sets: refinements of the radiative transfer model and the input data. *J. Geophys. Res. Atmos*. 109(D19105) doi:10.1029/2003JD004457.

Address reprint requests to:
Nancy Y. Kiang
NASA Goddard Institute for Space Studies
New York, NY 10025

E-mail: nkiang@giss.nasa.gov